Anti Coincidence Detector Requirements and Implications for the GLAST Trigger and Rates

Jonathan F. Ormes
with Cathie A. Meetre, Alexander A. Moiseev, Jay P. Norris,
Steven M. Ritz, Jeff M. Silvis and David J. Thompson

99.6.2

Overview

In GLAST, the requirements for background rejection and rate control are system-wide requirements and all subsystems play a role. In determining the requirements for the Anti-Coincidence detector, we need to understand the various fluxes involved and the functional approach to triggering GLAST. Previous studies of these effects have focused on the proton background and the efficiency of detecting photons. It has recently been pointed out that for studies of photons, eliminating the electron background is the dominant and driving requirement.

This note thus:

(1) determines a specification for background rejection that takes into account cosmic-ray electrons;

(2) summarizes the logic suggested for use in the GLAST trigger, and

(3) determines the cosmic ray integral and differential fluxes and estimates the L1 and L2 trigger rates.

A more efficient L2 trigger, taking advantage of the full ACD and tracker information in a single module is indicated by this study.

Methods for removing the residual backgrounds that are not removed by the L1 and L2 triggers and remain to be dealt with during Level 3 on-board software and ground processing are being developed by Norris et al. at GSFC and Burnett et al. on the west coast. We will present our approach to the ACD design including the study of gamma-ray lines in a separate note.

Background rejection

The scientific requirement that drives the instrumental background rejection requirement is the study of the diffuse high-latitude background. We need to separate the contribution from point sources and find out if there is any residual diffuse emission. To make progress on this problem, we *require* that the background due to charged particles be less than 10% of this signal. Our goal is to make the background an order of magnitude lower still.

For setting background rejection criteria, we care about both integral and differential fluxes of protons and electrons (Figures 1a and 1b). The most problematic decade is that between 3 and 30 GeV. At lower energy, at least outside the radiation belts, the geomagnetic cutoff reduces the cosmic ray rates dramatically. As long as we do not operate inside these belts, the very soft electrons found there will not be of concern. At higher energies, the cosmic ray fluxes fall faster than the gamma-ray fluxes.

The *incident* CREME proton spectrum peaks between 5 and 15 GeV and falls rapidly down to 3 GeV, but the spectrum of *measured* energies is approximately flat in numbers of particles per decade down to 100 MeV. The peak intensity (of the measured spectrum) is reduced by approximately a factor of 10 (compared to the incident spectrum). See Figures 2, 3, 4, and 5. Figures 2 and 3 (4 and 5) illustrate incident and measured spectra, respectively for protons (electrons).

The maximum integral proton flux (at solar minimum) is 2×10^5 times the diffuse high latitude photon flux (above 3 GeV) at the lowest vertical cutoff in the 28° orbit. This high flux is only present for a small part of the orbit. The minimum flux ratio is almost an order of magnitude less where the cutoff is about 15 GV. In addition, the efficiency for the calorimeter to capture the energy of the proton is low. Only 6% deposit more than 30% of their energy, 20% more than 10% of their energy, 26% more than 5% of their energy and 37% more than 1% of their energy. The distribution is quite broad for those protons with a reasonable track length in the calorimeter as can be seen in Figure 3. Combining the information in Figure 3 with that in Figure 1, we find the ratio of protons that deposit energy > 3 GeV in the calorimeter to the diffuse high latitude photons of 3 GeV and above is about 6×10^3.

Differentially, the proton problem is less severe because the proton spectrum is steeper than the extrapolated diffuse high-latitude gamma-ray spectrum shown in Figure 6. At the same energy protons outnumber the photons by 2×10^5 but at ten times higher energy, protons are less abundant by a factor of almost 200 making the operative ratio ~ 10^3. The integral requirement is the more severe.

There are many additional handles that one can use to reject protons. The tracks will be straight if there is no interaction, and when there is an interaction there will often be prongs in the tracker that give a topology quite different from that of a pair conversion. The calorimeter is another powerful discriminator against protons. Most of those that interact in the calorimeter will produce showers that look nothing like an electromagnetic cascade. Reaching the required rejection against protons is the easy part of the job. GLASTsim (Bill Atwood, Norris et al. private communications)

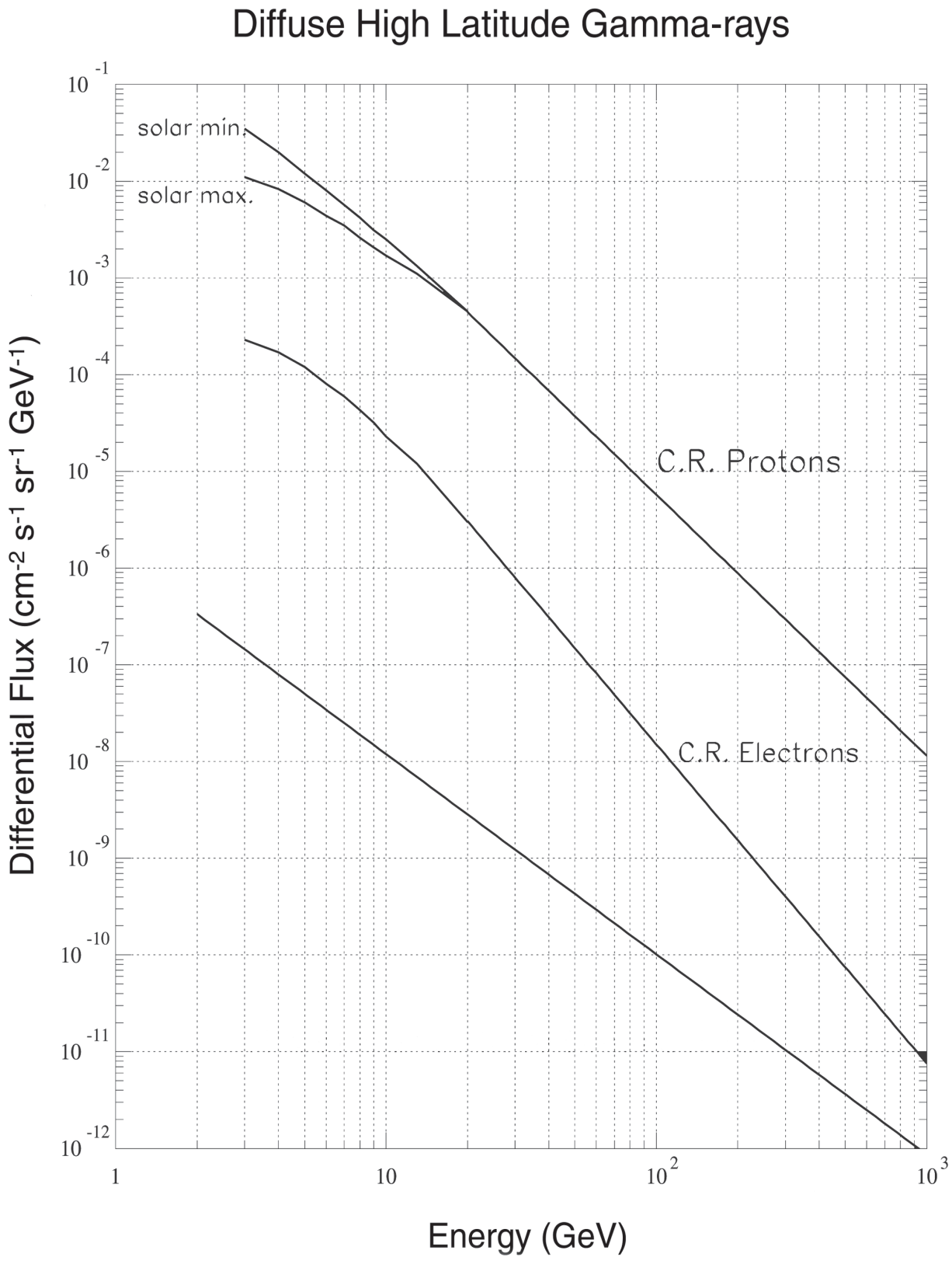

Figure 1a: A comparison of the fluxes of protons, electrons and diffuse high latitude photons (Differential representation).

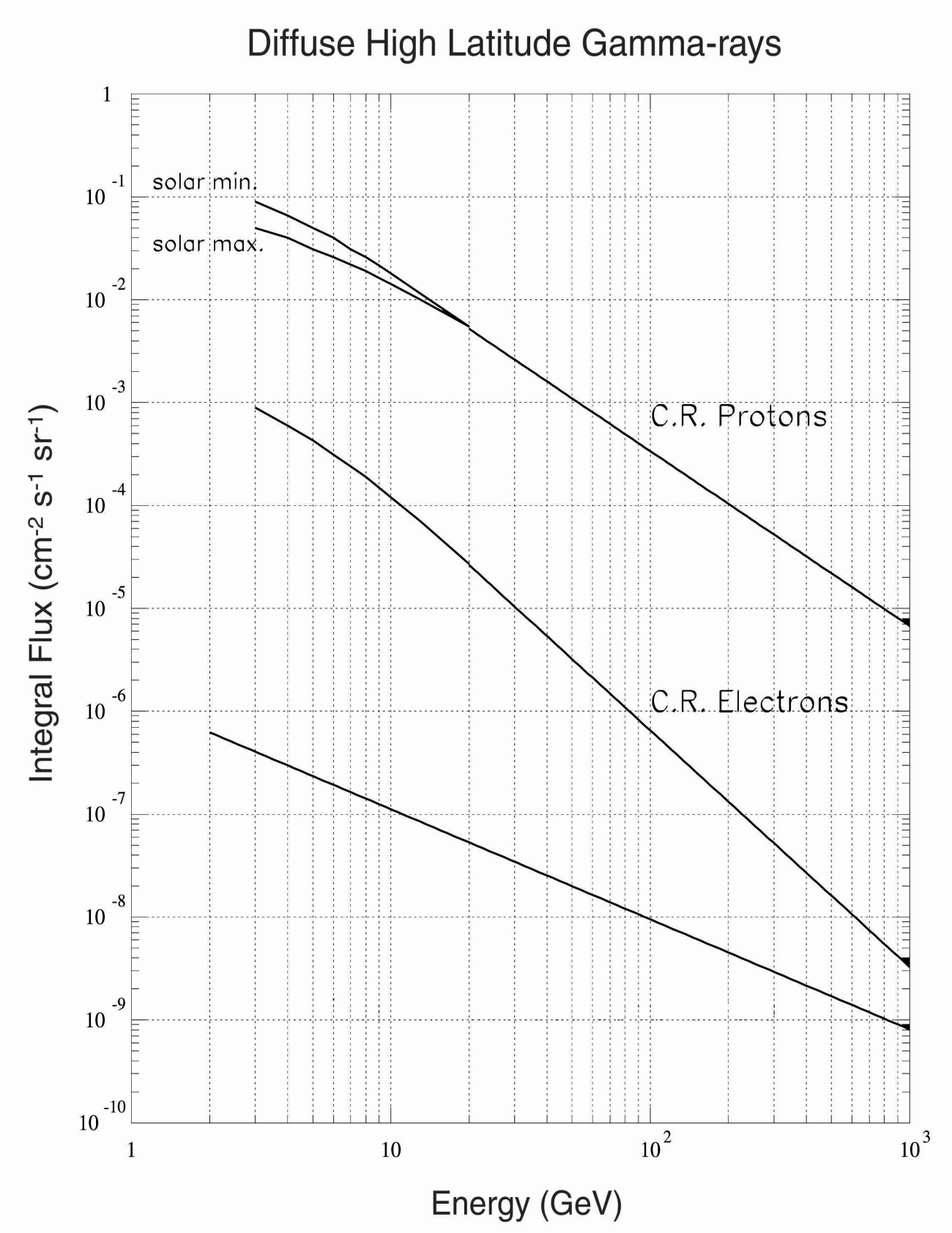

Figure 1b: A comparison of the fluxes of protons, electrons and diffuse high latitude photons (Differential representation).

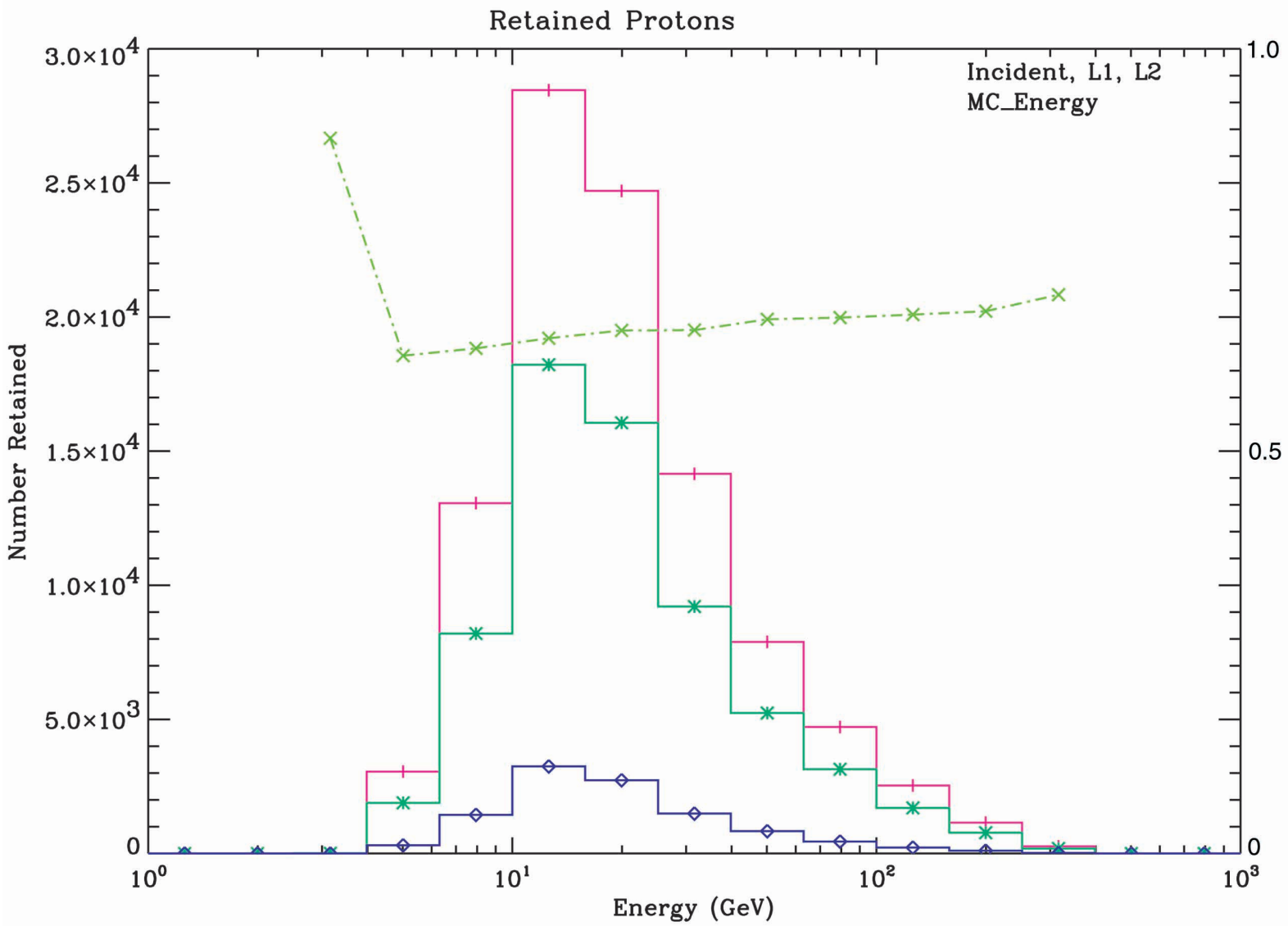

Figure 2: Simulated protons in GLAST as a function of the Monte Carlo truth energy. Different curves represent different event selections indicated. The ratio of the L1 rate to the incident rate is shown as the green dot-dashed curve with the scale at the right.

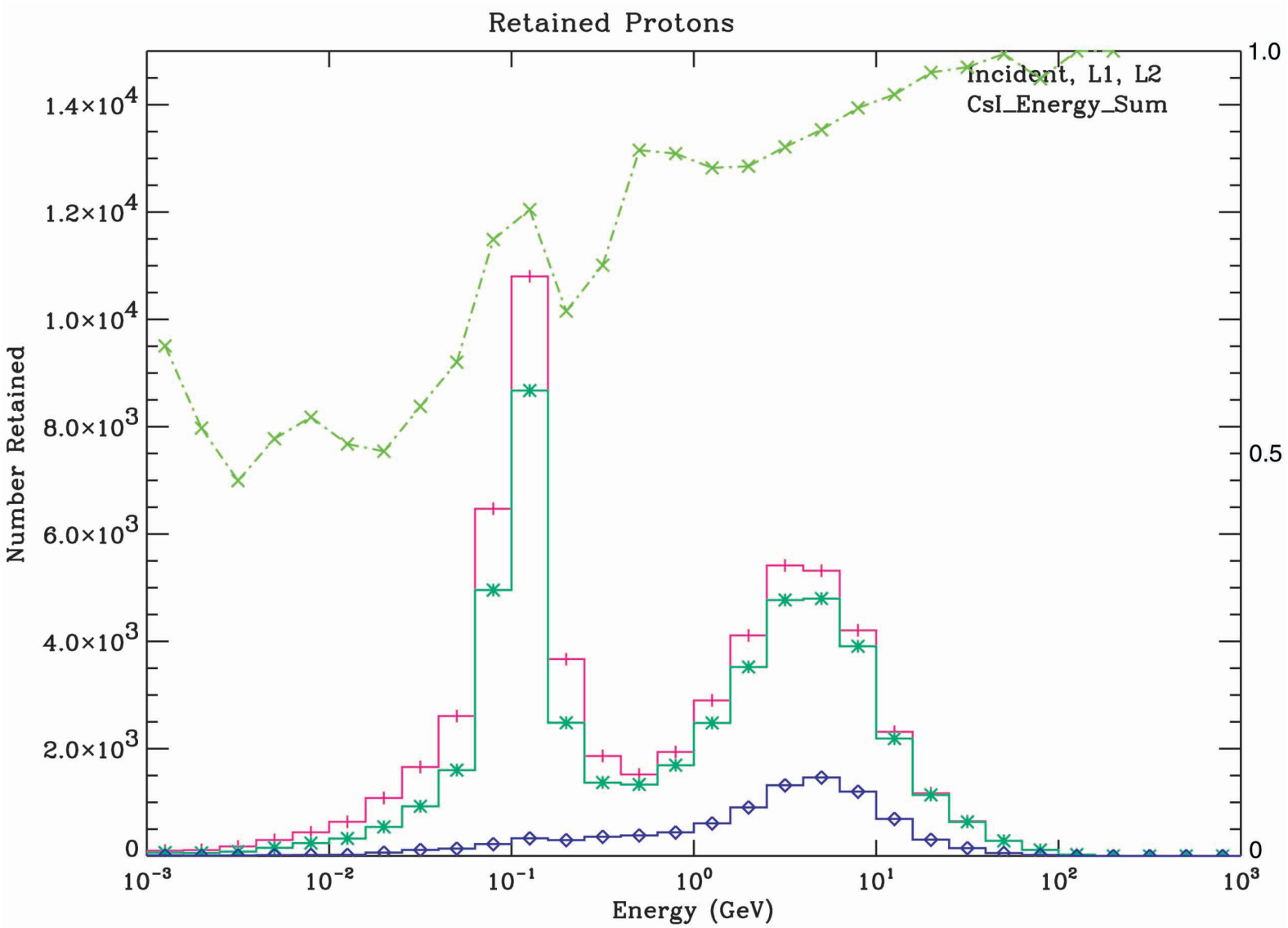

Figure 3: Simulated protons in GLAST as a function of the simulated "measured" energy. Different curves representing different event selections are indicated. The ratio of the L1 rate to the incident rate is shown as the green dot-dashed curve with the scale at right.

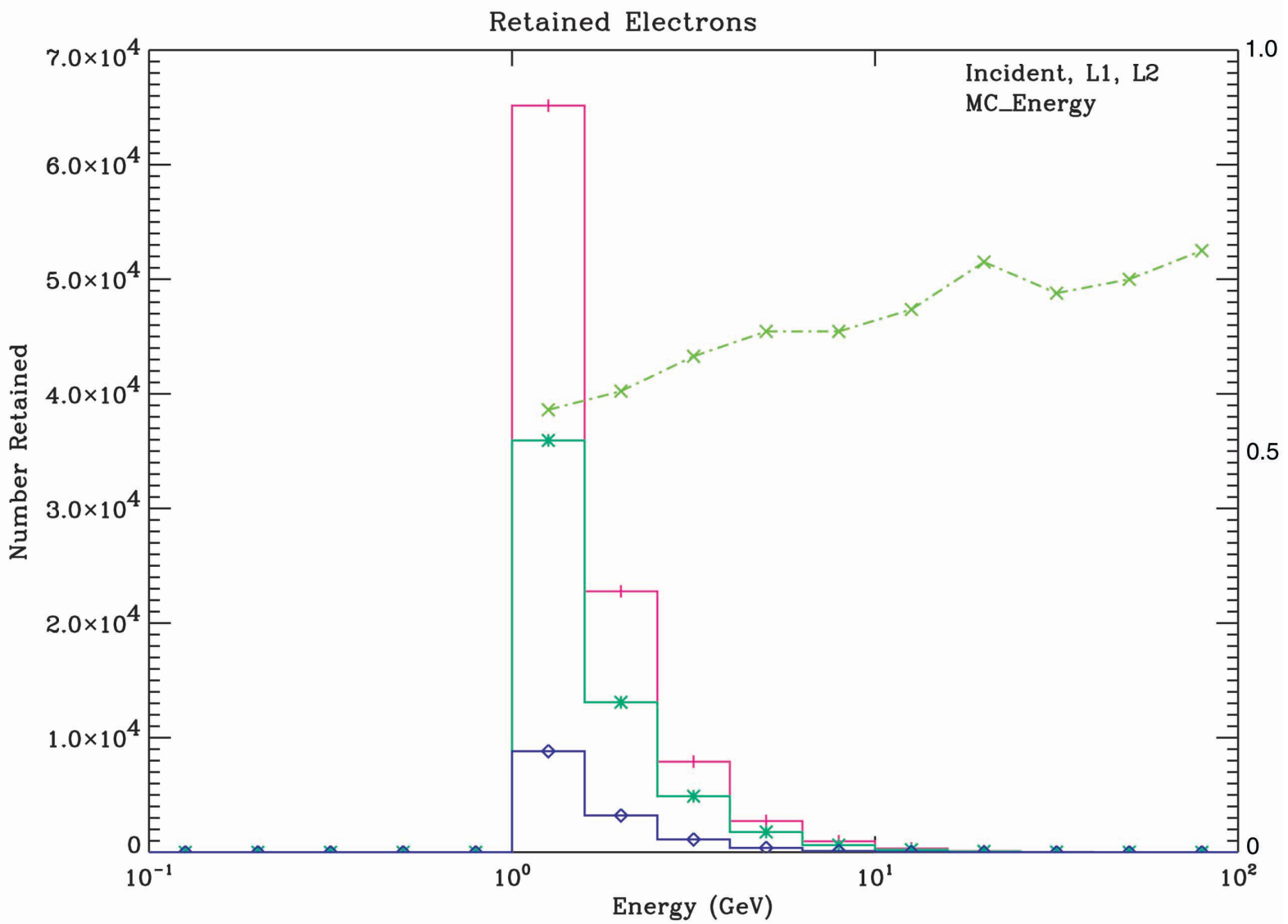

Figure 4: Simulated electrons in GLAST as a function of the Monte Carlo truth energy. Different curves representing different event selections are indicated. The ratio of the L1 rate to the incident rate is shown as the green dot-dashed curve with the scale at right.

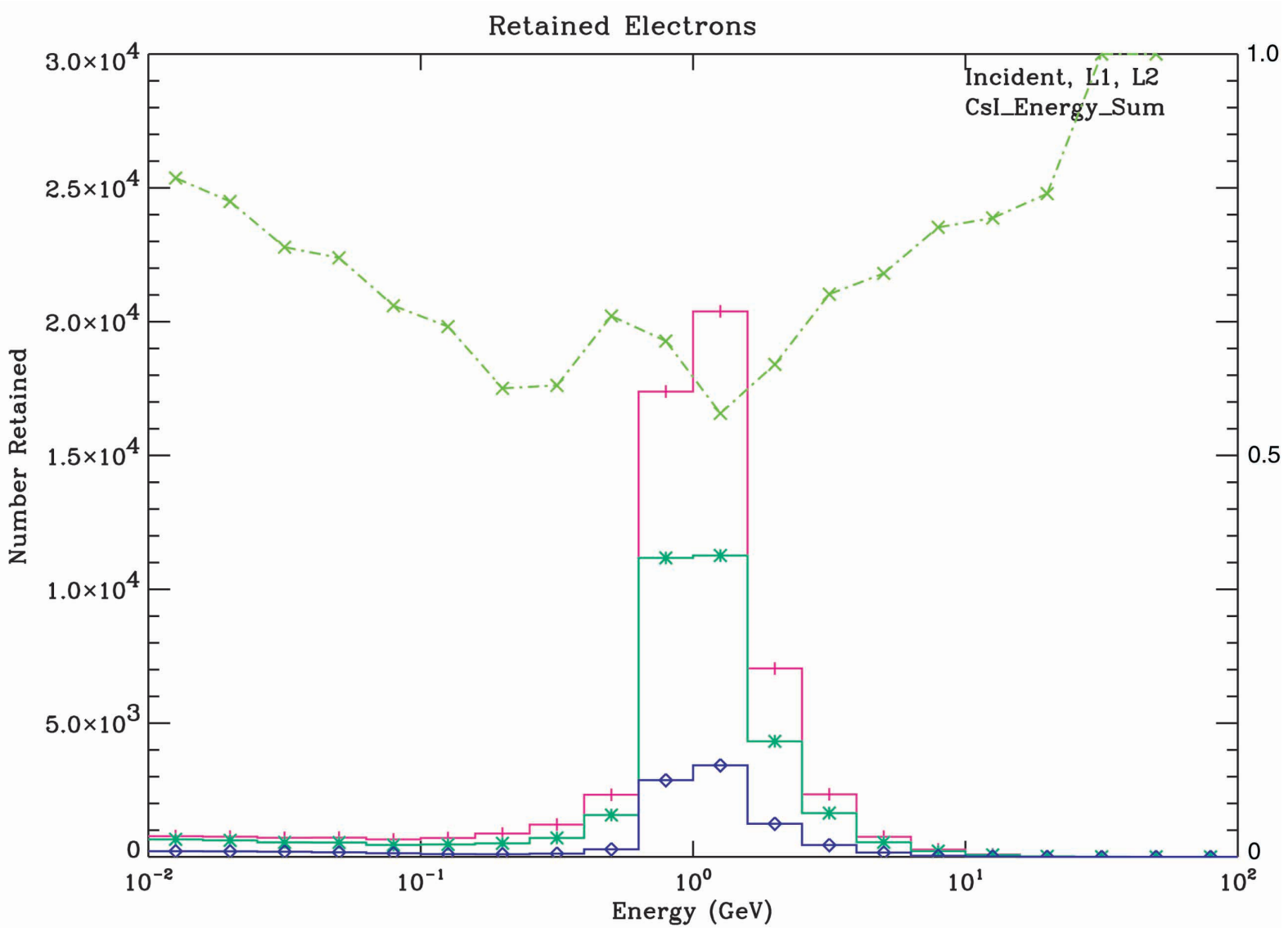

Figure 5: Simulated electrons in GLAST as a function of the simulated "measured" energy. Different curves representing different event selections are indicated. The ratio of the L1 rate to the incident rate is shown as the green dot-dashed curve with the scale at right.

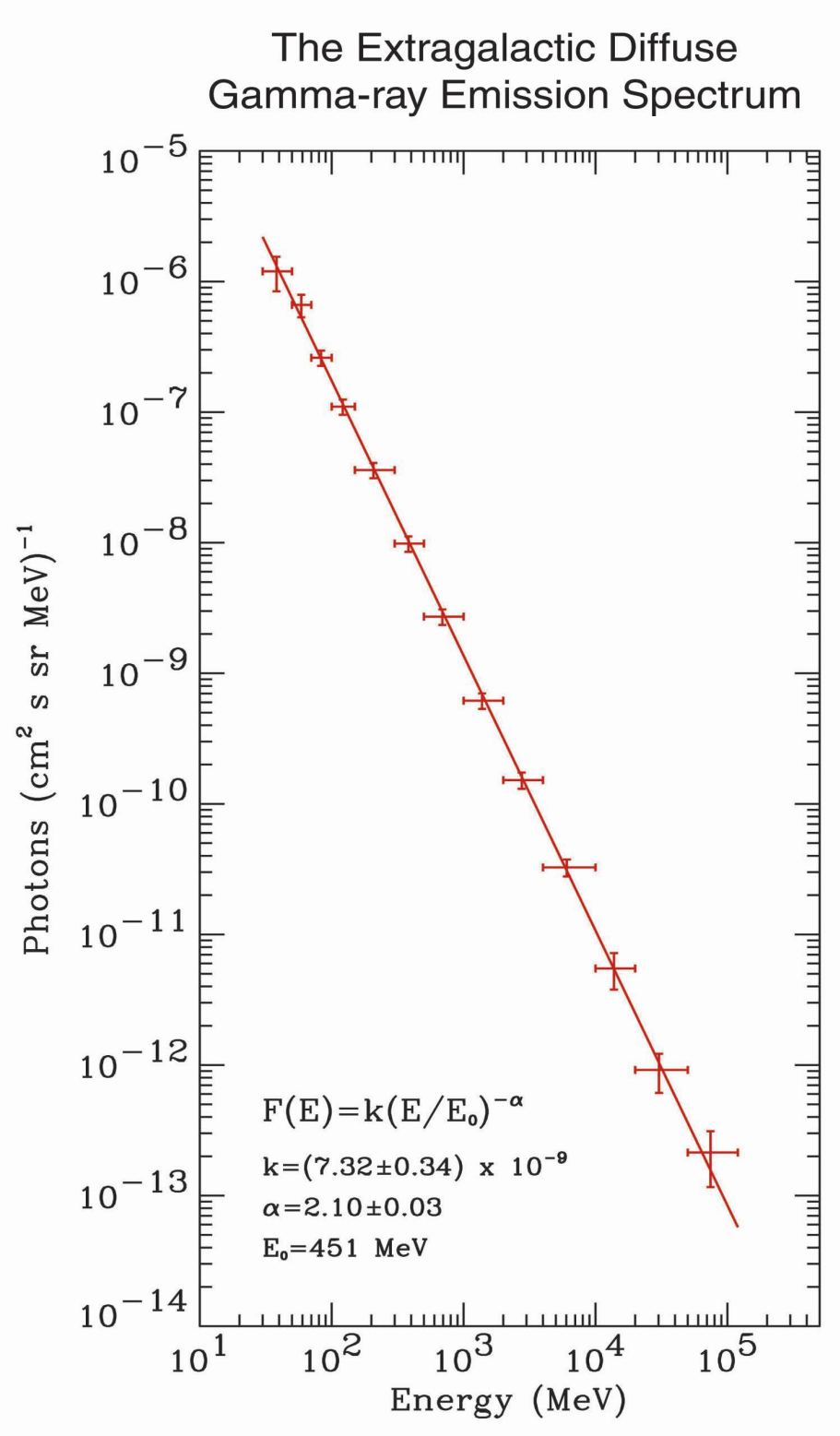

Figure 6: The extragalactic diffuse gamma-ray emission spectrum from Sreekumar et al., ApJ, 494, 523 (1998):

Differential: $I(E) = 1.4 \times 10^{-6}\ E^{-2.1}$ (cm^2 s sr GeV)$^{-1}$

$I = 7.32 \times 10^{-9}\ (E/451\ \text{MeV})^{-2.1}$ (cm^2 s sr MeV)$^{-1}$

Integral: $I(E) = 1.3 \times 10^{-6}\ E^{-1.1}$ (cm^2 s sr)$^{-1}$

studies have shown that the required levels of proton rejection can be met with an ACD that reduces the background by three orders of magnitude.

The integral electron flux at 4 GeV is 1% of the proton flux (see Figure 1). Allowing for the different cutoff energies for protons and electrons, we can use a worst case flux of 10 electrons/(m^2 sr s). At the same energy the integral diffuse gamma-ray flux is 3×10^{-3} photons/(m^2 sr s), a ratio of 3300. To achieve a residual electron flux of less than 10% of the diffuse gamma ray flux, we have to reduce the misidentified electron fraction to $< 3 \times 10^{-5}$ of the electrons.

Looking at the electron background problem as a function of energy, we see that the ratio of electrons to diffuse high-latitude photons peaks at 3000 between 3 and 10 GeV. For this energy range we need the misidentified fraction to be $< 3 \times 10^{-5}$. Above 100 GeV there are no measurements of the photon spectrum, but if the EGRET (Sreekumar et al. 1998) power law of $E^{-2.1}$ is extrapolated to 300 GeV the ratio of electrons to photons will fall to 40. Thus, the requirement[1] $< 3 \times 10^{-5}$ will work for all energies. Above 20 GeV the requirement drops to 10^{-4}.

For electrons it is much more difficult to use the tracker and the calorimeter to help in the rejection. In the calorimeter the showers will be identical to those of photons at the same energy; no help here. In the tracker, there are also problems. Naively, one might consider using the high spatial resolution to see the pair opening or the time over threshold to separate 1 from 2 track events, but a few minutes with GLASTsim will convince one that this is problematic. Electrons make bremsstrahlung photons easily and these convert creating extra tracks. Perhaps we can make the pattern recognition sophisticated enough to reduce the electron background by some TBD factor. Robert Johnson et al. (UCSC) have looked at using "time-over-threshold" near the conversion point and do not think it will help us much. At low energies, the Surplus_hit_ratio is useful against electrons. There will be slight differences near the starting point of the showers in the tracker but they will be difficult to measure and exploit. To work out something may be possible; in any case the exploration will take considerable effort and time. We should "keep this in our back pocket" and if possible, use this handle to help us go from "requirement" to "goal".
We can always add the outermost (usually the top) tracker layer (or region for side entering events) to obtain an independent verification that the event is not an electron

[1] Note that for much of the orbit, the ratio is a factor of 3 smaller and so we could live with some (TBD) decrease in sensitivity (i.e. use a restricted data set) if necessary.

that escaped detection. A single tracker layer is highly efficient but only covers 90% of the area. This would reduce background by a factor of 10. This will be simulated to determine the reduction in effective area. (The relatively small area on the side between the top of the calorimeter and the last converter layer has special problems that will be addressed elsewhere.)

In flight, we can also use the high precision tracking to map the spatial distribution of straight tracks that leak through the ACD to see if they come preferentially from "cracks." If they are due to statistical fluctuations in the collection of the light in the scintillators, they will be distributed uniformly. If cracks are problematic, events that might have come through those regions could be rejected. Cracks should be avoided if possible because they will result in a loss in efficiency that is energy dependent. At high energies, the tracks are relatively straight, making the loss minimal, but at low energies the losses would be larger.

Based on the considerations discussed above, we set the GLAST system level design *requirement for the misidentification of charged cosmic rays to be* 3×10^{-5} or a detection efficiency of 0.99997, and the *goal to be* 3×10^{-6} or 0.999997. <u>The electron component drives the requirement for the ACD to have 0.9997 efficiency.</u> We can expect one "9" from the top tracker layer (only necessary for studies where any residual background is critical) to meet our requirement. The goal of five and a half "9"s will be met if we can find one "9" from "pattern recognition" of the difference between photons and electrons in the tracker layers or do better with the ACD.

The ACD will have the same rejection power for protons as for electrons, so the false gamma-ray rate from protons should be below that for electrons.

We have separated the efficiency and hermeticity specifications. The tracker cannot protect us from inefficiency, but it can help with leakage. We can make the leakage comparable to the inefficiency by offsetting the cracks between ACD tiles from tower boundaries. For events where background elimination is most critical, the top tracker layer can act as part of the charged particle identification system and will "cover" the cracks.

How well we accomplish the rejection of charged particles can be verified in flight. We can study the residual diffuse high-latitude gamma-ray background as a function of vertical cutoff rigidity in the orbit or of some other comparable variable that is representative of the cosmic ray rate (e.g. "3-in-a-row" Level-1 triggers).

In summary, the first line of defense against charged particle backgrounds will be the ACD. For protons, internal pattern recognition using the tracker and calorimeter data can and should provide additional protection. This implies that the ACD must be 0.9997 efficient and have leakage $< 3 \times 10^{-4}$. Because of the high-resolution tracking, we can afford to have cracks of known location that leak at a higher level, but we will design to minimize them. If cracks leak particles through with probability $> 3 \times 10^{-4}$, they will represent a slight energy-dependent inefficiency for photons (and worst at low energies where the angular resolution is poorest).

Suggested GLAST Trigger Baseline

A "3-in-a-row" trigger or "$E_{cal} > E_{low\text{-}threshold}$" in any tower is an L1 trigger that initiates decision making:

(1) Is "$E_{cal} > E_{low\text{-}threshold}$"? Is calorimeter E_{cal} > some threshold in a tower? Two threshold levels will be required if we want to accept the highest energy events irrespective of the status of the ACD. [The lower threshold is currently being implemented (in GLASTsim) by having more than 100 MeV in a single crystal in a single tower. This retains >90% of gammas with E > 1GeV while eliminating 40% of the protons. Using 3 crystals instead has a 20% effect on the proton rate, but decreases the gamma efficiency similarly.]

(2) Is there a reasonable track, and if so, did the "indicated ACD tile" (to which the track points) fire? It will be Level 3 where "noise" events can be separated from low-energy (highly scattered) photons, limb photons, etc. We explore the implementation of this trigger in more detail below. Events for which there was either a "3-in-a-row" or "$E_{cal} > E_{low\text{-}threshold}$" but there was no definable track should be dealt with at L3 or beyond. Given this philosophy we construct the following logic for the trigger:

<u>From L1 we get:</u>

"3-in-a-row" = **3**; otherwise **.not.3**

ACD Low Z threshold exceeded = **ACD**; otherwise **.not.ACD.aud.Hi-Z threshold not exceeded**

ACD Hi-Z threshold exceeded = **Z**; otherwise **.not.Z**

"$E_{cal} > E_{low\text{-}threshold}$" (~1 GeV) .and. "$E_{cal} < E_{high\text{-}threshold}$" (~20 GeV) = $\mathbf{E_{low}}$; otherwise, $\mathbf{.not.E_{low}}$

"$E_{cal} < E_{high\text{-}threshold}$" (~20 GeV) = $\mathbf{E_{high}}$; otherwise, $\mathbf{.not.E_{high}}$

<u>At L2 we combine the ACD with the tracker:</u>

Does "3-in-a-row" have a reasonable (low χ^2) track?

No: pass event to L3.
Yes: Does that track point to an ACD tile which was hit?
[The hit ACD hit array is not filled if Hi-Z discriminator fires.]

Yes - global[2] **veto** of event
No - pass event to Level 3

Thus events entering Level 3 include five types:

(1) "$E_{cal} > E_{low\text{-}threshold}$" (~1 GeV) events with no track pointing to an ACD tile with a hit (**.not.3** .and. $\mathbf{E_{low}}$)
(2) Three-in-a-row events with a track, but that track does not point to a hit ACD tile (**3** .and. **.not.ACD**)
(3) Three-in-a-row events with a track, but that track does not have low χ^2.
(4) "$E_{cal} > E_{high\text{-}threshold}$" (~20 GeV)
(5) High Z events (**Z**)

• Type 1 includes the "calorimeter only" high-energy photons. At high energy there can be ACD hits, but they should pass because there is no track to point back to the hit tile.
• Type 2 includes photons that converted in the tracker. There should be little bias against low-energy highly-multiple-scattered photons passing to this level.
• Type 3 should include noise, highly-multiple-scattered photons.
• Type 4 are the highest energy events that we wish to keep irrespective of the status of the ACD, track quality, etc. Obviously we want the photons even if there is backsplash. I have not been able to think of anything worthwhile to do with the hadrons which pass this trigger that has not been done before. But the study of 20 to 1000 GeV electrons is worthwhile as a sideline. We can adjust the threshold (20 GeV) if the rate of this kind of event is too high.

---

[2] Except for Hi-Z (= **Z**) and "$E_{cal} > E_{high\text{-}threshold}$" ($\mathbf{E_{high}}$)

• Type 5 are for calibration. We may want to select a subset at level 3 or prescale these triggers.

The L2 global **veto** using the ACD takes care of the rate. It eliminates double tower triggers, and those background events with energy deposit between 1 and 20 GeV that give both "3-in-a-row" pointing back to a hit tile and an E > 1 GeV in the calorimeter.

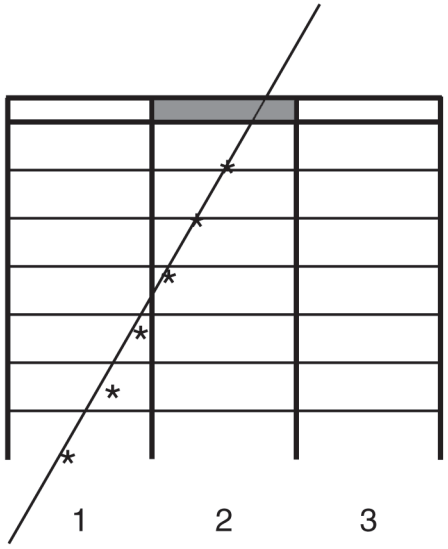

In the diagram, at the left, tower #2 is "topmost" and can be rejected by L1 or L2 trigger, but tower #1 gives unwanted trigger. These events are eliminated at L2 where any tower with ACD kills the event "global" veto.

Rationale: In this approach, L2 is done in software at the single-tower level. If this is not done at L2, these "other tower triggers" will dominate the rate entering L3. The calorimeter and tracker data do not need to be combined to carry out the L2 trigger functions. Except for specialized triggers (Hi-Z or High-E), any vetoed event will veto all towers so that even if more than one tower triggers, the event is killed. This takes advantage of the fact the cosmic ray background tracks will be straight, and that at L2, we have the map of tile hits available at all the towers. Decisions about track quality at this level should be simple and will not require knowing the spacecraft attitude. More complex analysis can be done at Level 3 if desired. This trigger prevents us from inadvertently throwing out low-energy photons that scatter a lot at Level 2. This method should be designed to throw out only events that are clearly background, deferring to Level 3 or ground analysis the process of eliminating other undesirables such as limb photons, noise triggers, etc.

There will be "messy" events from protons which (hadronically) interact, sneaking through L2, but as long as the rate of these is not too bad, they can easily be killed at L3. The rate leaving L2 will have most (~90%) of the cosmic rays eliminated. Those sneaking through will have confusing or incorrectly projected tracks. Upward

moving cosmics that interact may be hard to get rid of, so there may also have to be a L2 cut on "too many hits" in a tower. We should check this for pointed observations for which the bottom of the calorimeter is exposed. If any tower at L2 can kill the whole instrument, those that trigger more than one tower do not get through if one tower "votes no." We need to check the rates coming out of L2; I assume they will be dominated by interacting protons and next by albedo and limb photons.

At high energy where photon tracks are straight, the calorimeter controls the triggering rates. We can and should have some adjustment on the calorimeter threshold energies.

In this scheme, "nearest neighbors," a superset of ACD tiles associated with and "covering" each tower, are only used at L1 for rate control in the case of trouble. The above trigger scheme is indicated in Figures 7 (a and b).

Rate Considerations

The best available proton flux data is shown in Figures 8 (a and b). This data is from the modern balloon-borne spectrometers LEAP (Seo, E.S., et al., ApJ, 378, 763, 1991), IMAX (Wolfgang Menn et al. XXV ICRC, Durban, 1997, 3, 409), and BESS (Tomoyuki Sanuki et al. presented to XXVI ICRC, Salt Lake City, 1999). These experiments give a differential flux of 20 particles/(m^2 sr s GeV) at 10 GeV. Be careful with this figure; note the flux axis is multiplied by the kinetic energy to the 2.5 power. Other data taken by various spectrometers show some measurements as much as a factor of 1.5 higher. The differential CREME spectrum gives 16 particles/(m^2 sr s GeV) at 10 GeV.

The vertical geomagnetic cutoff in a 28° inclination orbit will vary from just over 4 GV to around 15 GV over the orbit (Figures 9 and 10)[3]. The worst case integral flux at solar minimum at the lowest vertical cutoff in this orbit is 900 particles/(m^2 sr s) and it will vary down by almost a factor of 10 to ~100 particles/(m^2 sr s). This includes about 10% allowance for helium nuclei. The comparable number in Grove's note is 350 to 510 particles/(m^2 sr s) depending on the phase of the solar cycle. Grove's orbit average flux from CREME is 130 /(m^2 sr s). For reference, we include as Figures 11a and 11b, CREME spectra, differential and integral respectively, including fluxes in free space outside the magnetosphere, at longitude 285° on the orbit where the flux is maximal and the orbital average. Both proton and helium spectra are included.

[3] The minimum cutoff in 28° orbit is 4. GV rigidity (momentum per unit charge). This is 3.17 GeV for protons, 1.27 GeV/nucleon for A/Z = 2. This occurs at +28.° latitude and longitude 285°.

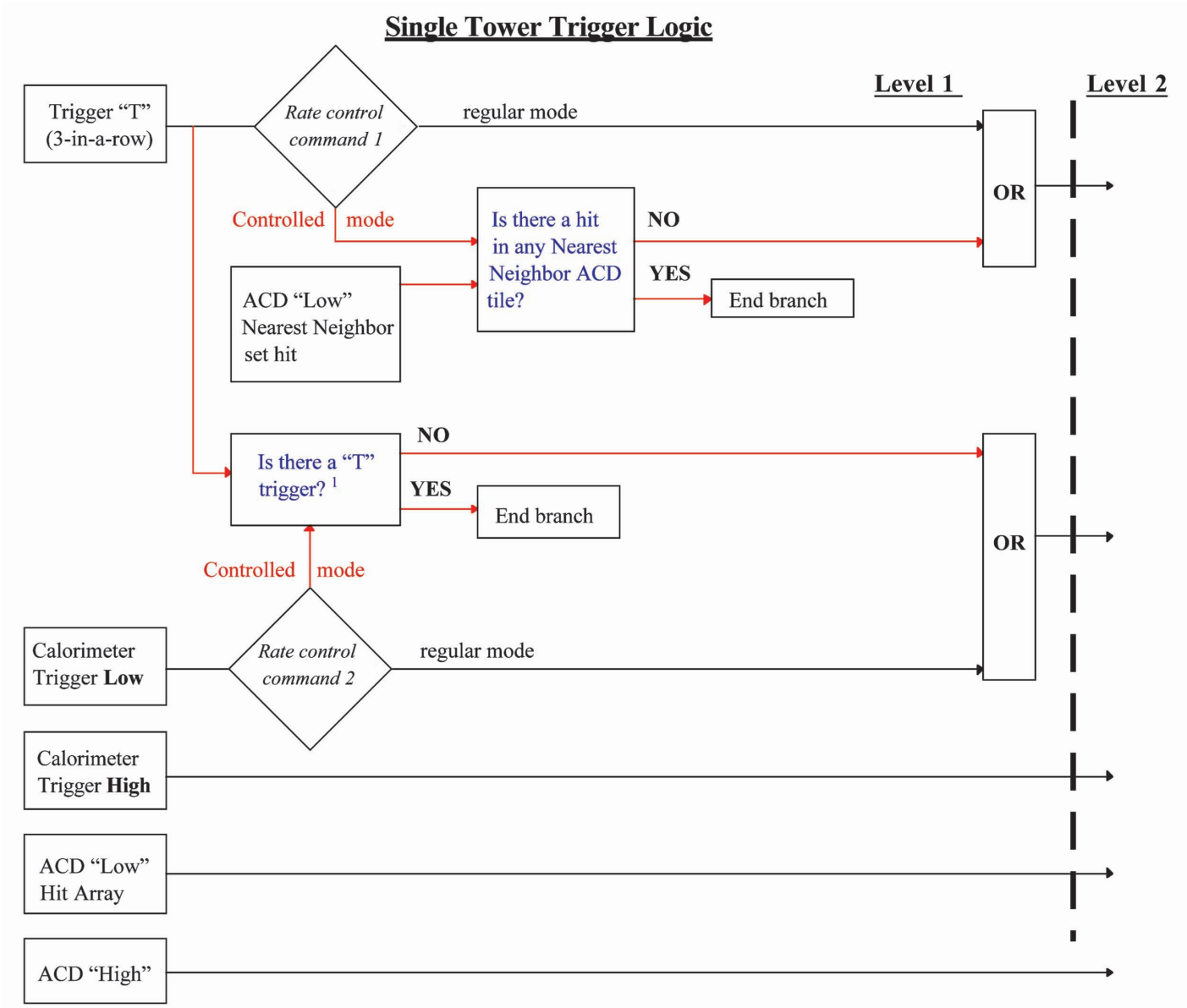

[1] There will be a loss of redundancy for the tracker-calorimeter cross check, but we want to keep "calorimeter only" events.

Figure 7a

Single Tower Trigger Logic

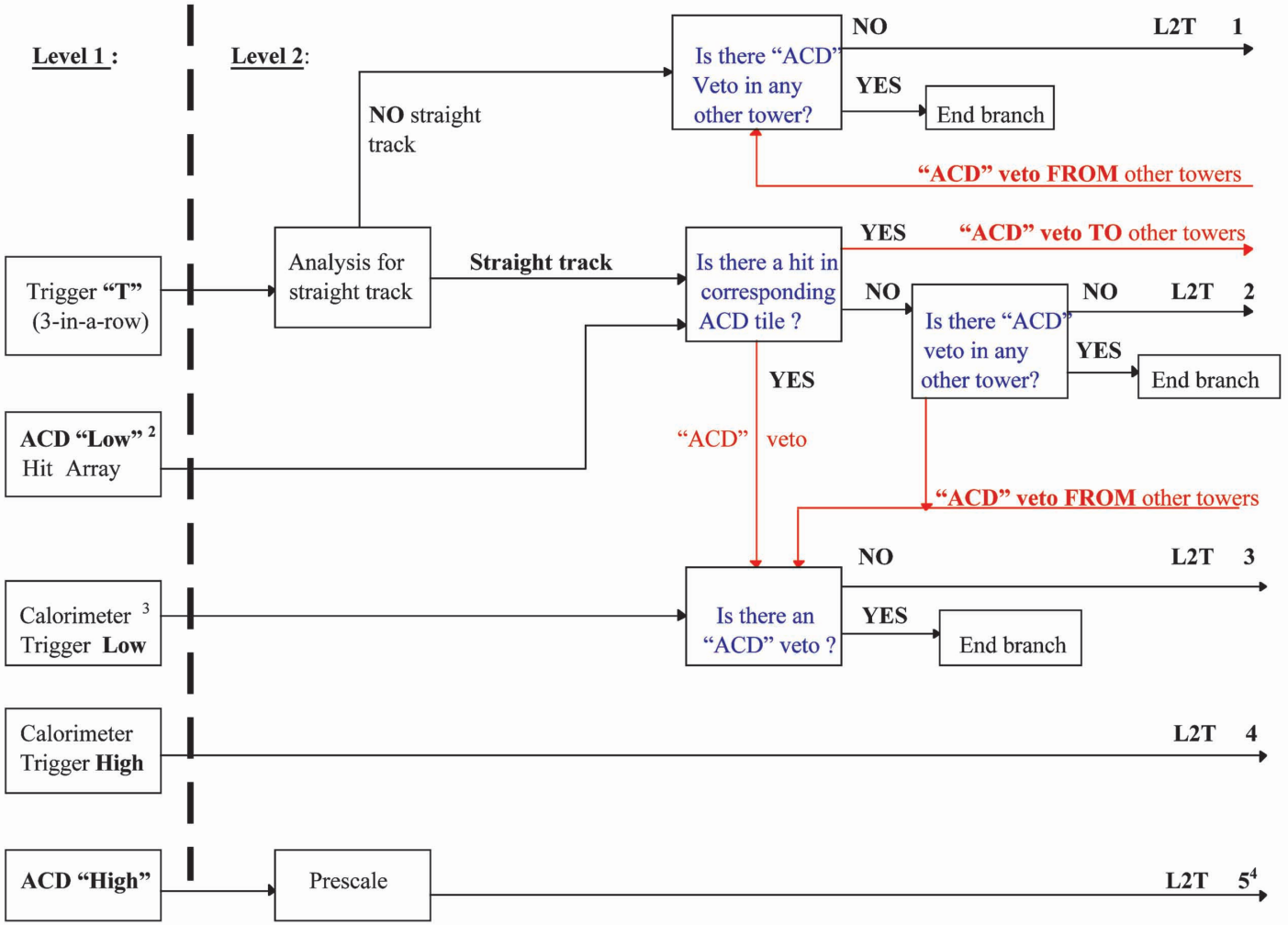

[2] An ACD Tile sends an ACD "Low" if and only if the tile fired a low level discriminator but not the high Z level.
[3] More than 100 MeV in a single crystal but does not fire the high level discriminator
[4] If all L2T bits are false, master reset

Figure 7b

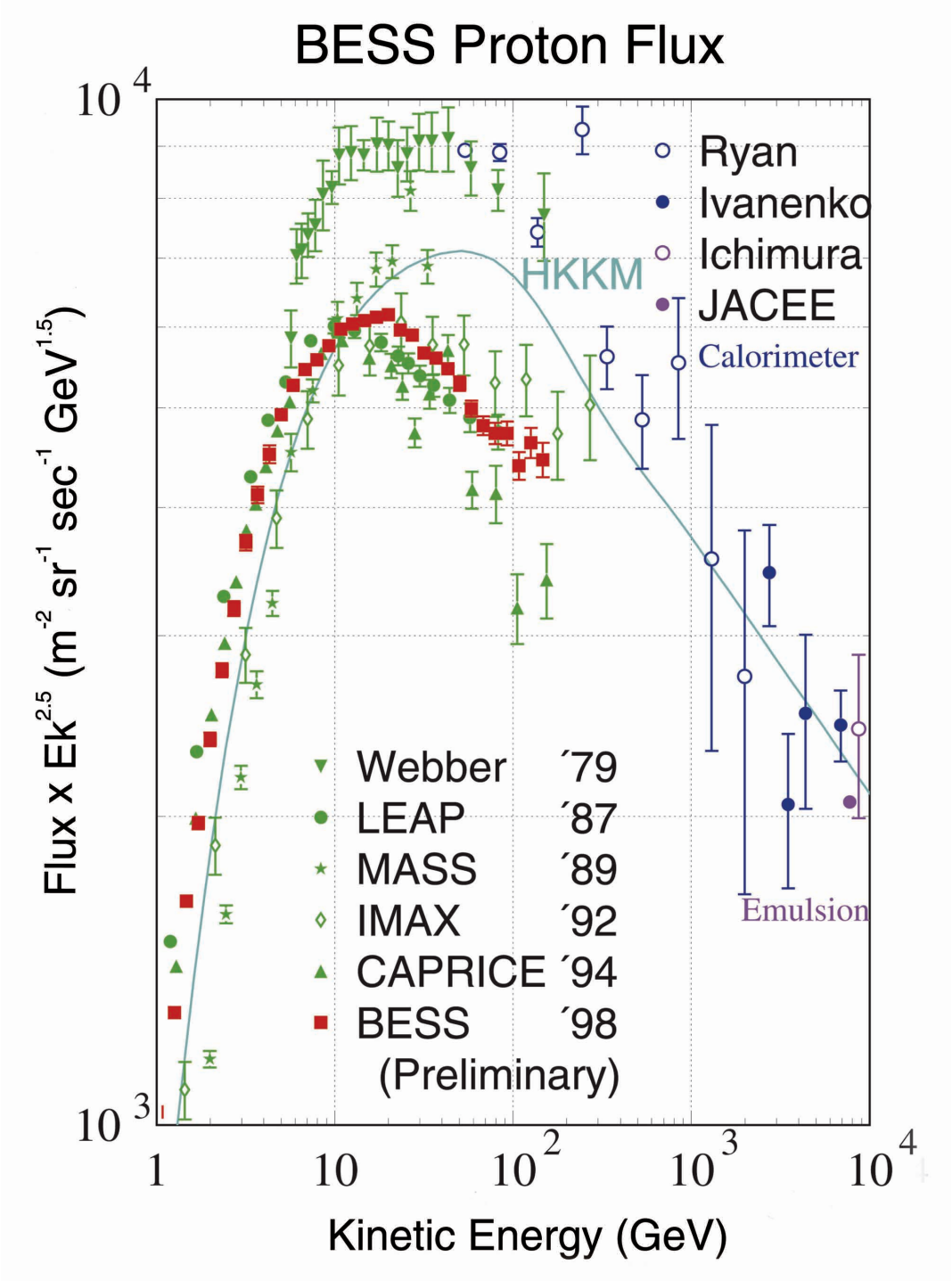

Figure 8a: The flux of cosmic ray protons measured on balloon borne platforms referenced below. The year the data were taken is indicated. Note the data of the magnet spectrometers IMAX, CAPRICE and BESS, flown during the 1990's.
References are: Seo, E.-S., et al. (LEAP), ApJ, 378, 763 (1991); Menn, W., et al. (IMAX), XXV ICRC, 3, 409 (1997)
Differential: $I(E)=1.44E^{-2.7}$ $(cm^2\ s\ sr\ GeV)^{-1}$
Integral: $I(E)=0.85E^{-1.7}$ $(cm^2\ s\ sr)^{-1}$

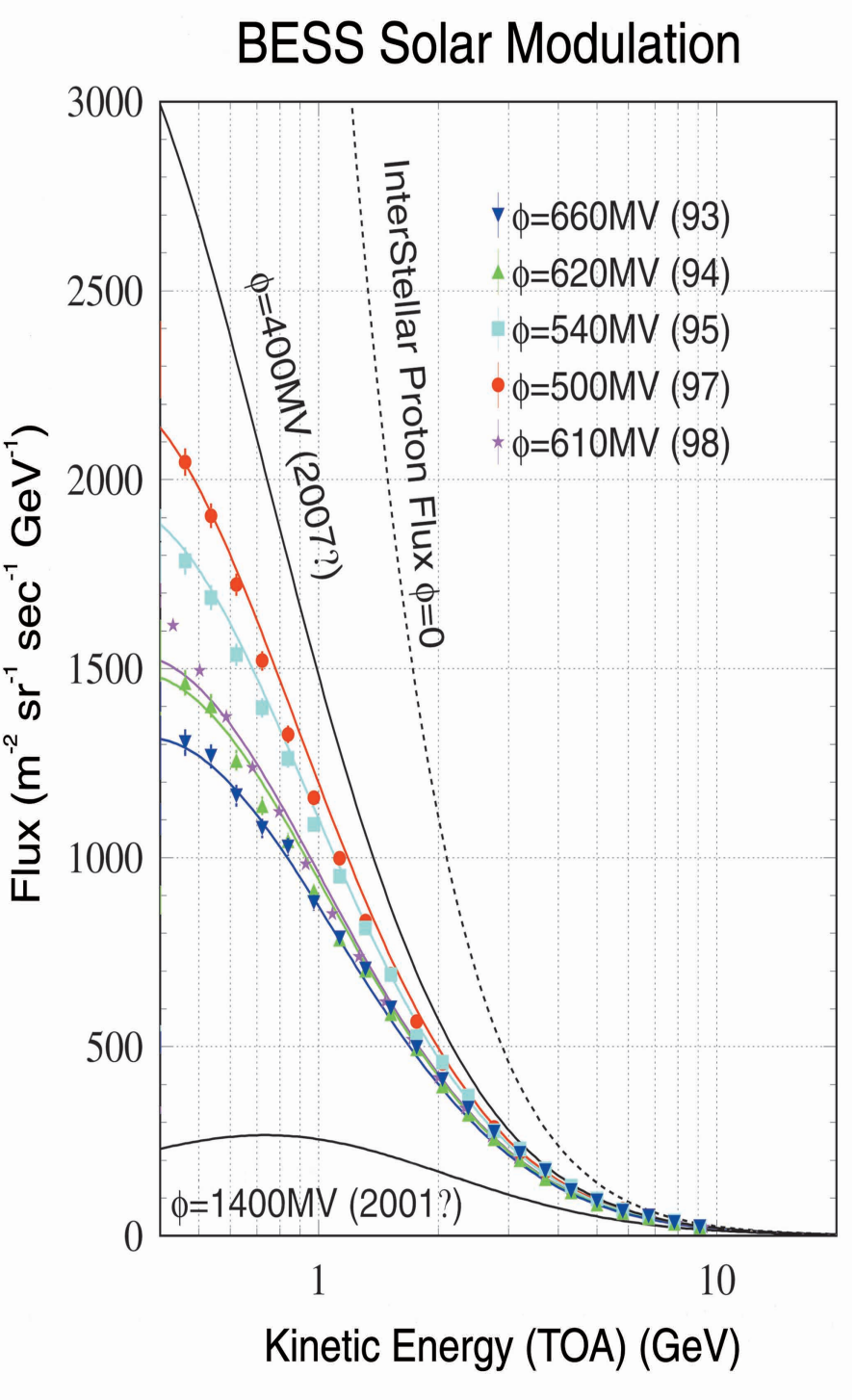

Figure 8b: The flux of cosmic ray protons measured on balloon borne platforms referenced below. The BESS spectra are shown above at different levels of solar modulation.

References are: Seo, E.-S., et al. (LEAP), ApJ, 378, 763 (1991); Menn, W., et al. (IMAX), XXV ICRC, 3, 409 (1997)

Differential: $I(E)=1.44E^{-2.7}$ (cm^2 s sr GeV)$^{-1}$

Integral: $I(E)=0.85E^{-1.7}$ (cm^2 s sr)$^{-1}$

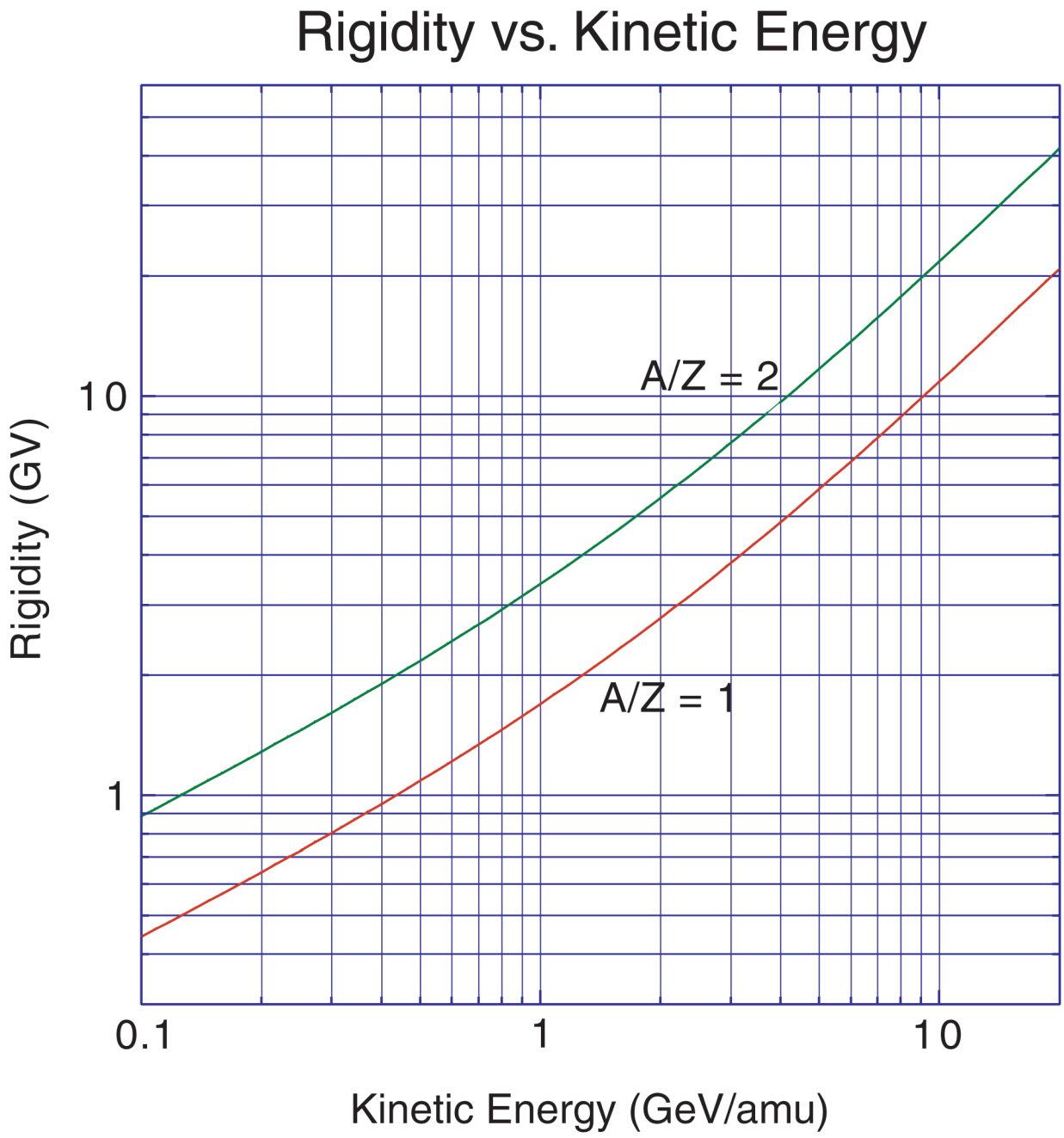

Figure 9 Conversion between magnetic rigidity and kinetic energy for particles with A/Z = 1 and 2.

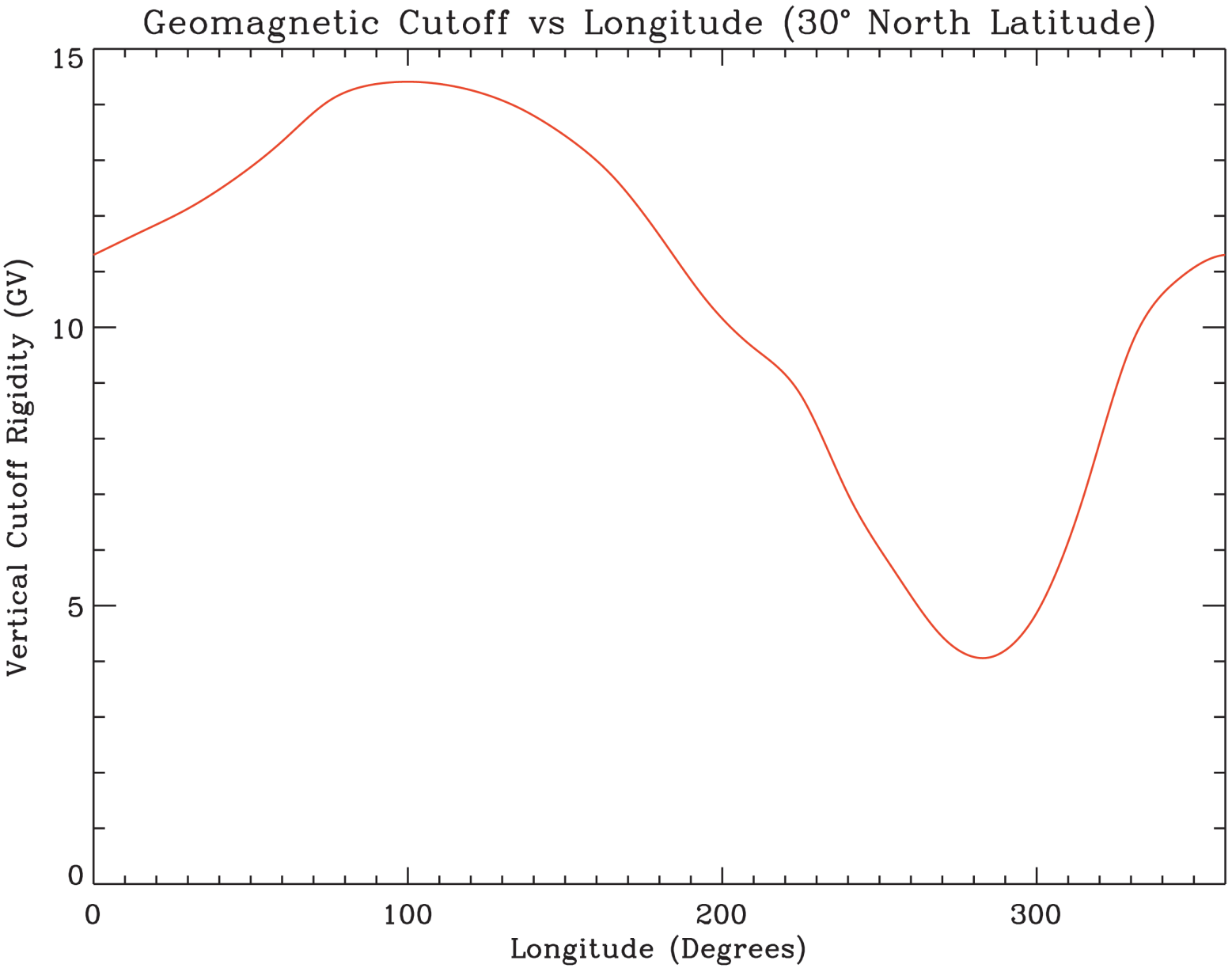

Figure 10: Geomagnetic cutoff as a function of longitude for 30 degrees north latitude.

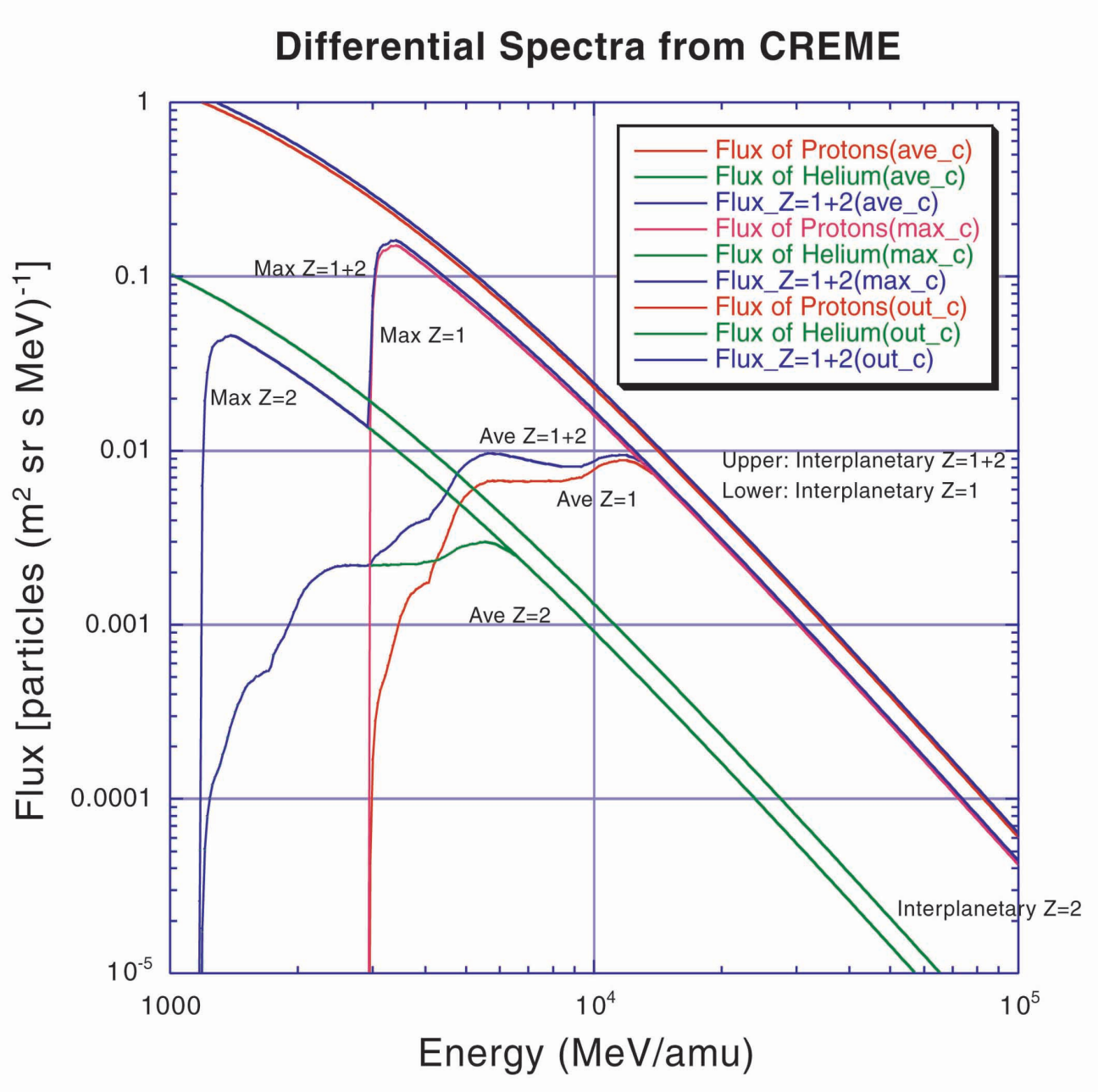

Figure 11a: This figure was generated by the CREME program. It includes the proton spectrum, the helium spectra and the summed spectrum in geosynchronous orbit outside the magnetosphere, in 28.5° 550 km circular orbit at 285° longitude corresponding to the minimum cutoff in the orbit and the orbital average spectra. This figure shows differential spectra computed using CREME.

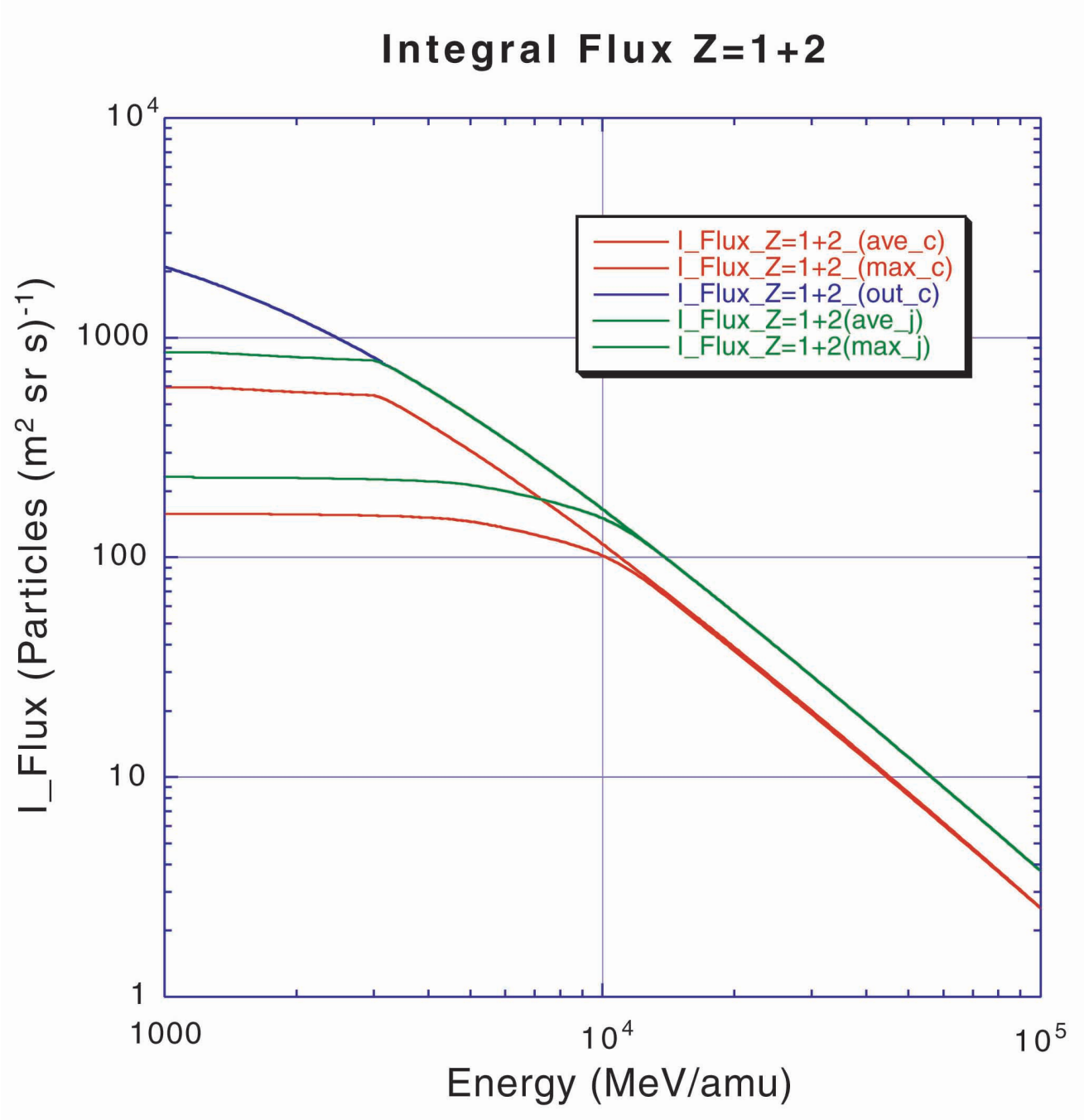

Figure 11b: This figure was generated by the CREME program. It includes the proton spectrum, the helium spectra and the summed spectrum in geosynchronous orbit outside the magnetosphere, in 28.5° 550 km circular orbit at 285° longitude corresponding to the minimum cutoff in the orbit and the orbital average spectra. This figure shows the integral spectra for the sum of Z=1 and 2 nuclei that were used to compute rates. The uppermost curves are integral outside the magnetosphere, the upper (lower) green curves are the maximum (average) in orbit corrected for the Earth shadowing (see text), and the red curves are the corresponding uncorrected curves that come directly from CREME.

We reconcile these fluxes as follows:

(1) The CREME/CHIME transparency of the geomagnetic field is $0.7 = 1.43^{-1}$ at the highest energy. I do not know why this is not 1.0. The measurements with which we compare are taken at balloon altitudes. The CREME spectrum at geosynchronous orbit agrees well with high-latitude balloon measurements. Earth shadowing should not be this large an effect for a zenith-pointed surface at energies well above the cutoff.

(2) A detailed comparison of the CREME fluxes shows that the peak flux on orbit is 4.8 (rather than the commonly used 4.0) $\times$ the CREME orbit average.

Note that $130. \times 4.8 \times 1.43 = 892/(m^2\ sr\ s)$, in good agreement with my rounded off number of 900 particles/(m^2 sr s).

To obtain rates we need some geometric factors:

The top surface of GLAST:

$1.7\ m \times 1.7\ m \times \pi\ sr = 9.08\ m^2\ sr$

The 4 side surfaces of GLAST, including the calorimeter, shadowed (0.74) by the Earth ($113° < \theta < 180°$):

$1.7\ m \times 0.83\ m \times 4 \times (0.74 \times \pi\ sr) = 13.1\ m^2\ sr$

The side of the instrument is divided into three zones covered by ACD and uncovered. (The last 3 tracker trays, not covered by the lower row of ACD tiles, is one of the more vunerable regions to electrons; level 3 discriminants must handle this region effectively; or possibly, the lower ACD tiles should be extended to cover it.) The three zones[4] are:

7.60, 2.39 and 3.10 m^2 sr

For events that pass through the top surface of GLAST and the bottom of the calorimeter (formula in Appendix A):

3.89 m^2 sr

---

[4] The top zone is from the top of the side down to the last converter plate, the region covered by the baseline ACD. The second zone is the uncovered (by ACD) region from the bottom converter plate to the top of the calorimeter, and the third zone is the side of the calorimeter.

For events that pass through the top and bottom surfaces of the calorimeter (formula in Appendix A):

$7.27\ m^2\ sr$

The 4 side surfaces of the calorimeter with a track length of at least 0.2 m (formula in Appendix A):

$1.63\ m^2\ sr \times 0.74 = 1.21\ m^2\ sr$

And the shadowed calorimeter bottom:

$(1.7\ m)^2 \times 0.15\ \pi\ sr = 1.39\ m^2\ sr$

From these numbers we get the maximum event rate through the top of GLAST (a plane of area 1.7 m × 1.7 m has π sr [9.1 m^2 s]) to be 8.2 kHz. GLASTsim studies by Norris et al. show that 76% of these events make an L1 "3-in-a-row" trigger (6.2 kHz). The angular distribution of these events through the top and sides of GLAST are shown in Figures 12 (a and b). The uppermost curve is the zenith angle distribution of events through the top surface of GLAST (9.1 m^2 sr). The middle histogram is the 76% subset of these that make L1 "3-in-row" triggers, and 34% of those also trigger the calorimeter, but this fraction includes the probability of energy deposit above the trigger.

The rate through the sides of GLAST, taking $0.74^5 \times \pi$ as the solid angle including Earth shadowing, will be 11.8 kHz; 56% of these events make a either a "3-in-a-row" trigger or an "$E_{cal} > E_{low\text{-}threshold}$" (or both), giving a rate of 6.6 kHz. L1 triggers from the bottom contribute about 1 kHz. This makes the maximum L1 trigger rate about 14 kHz from charged cosmic rays. The comparable rate given by E. Grove in his 97.4.7 memo was 16 kHz. The minimum rates are an order of magnitude less than the maximum rates. We have not considered solar flares.

I estimate an orbit average rate as 12.7 kHz/4.8 = 2.9 kHz. The comparable CREME estimate would be 2.9 × 0.7 = 2.0 kHz. To be on the safe side, GLAST should be designed to handle a rate of at least 15 kHz and a 4 kHz average rate. [If I understand Toby's 98.7.5 memo, his number for the orbital average L1 trigger rate is 1.769 kHz. This corresponds to the 1.2 kHz number from Bill Atwood that is in common use.]

---

[5] For a GLAST pointing towards the local zenith, I have taken the geometric factor through a side surface to be 0.74 that of an equal area without side shadowing. As the instrument axis moves off the local vertical, one side gets more exposure while the opposite one gets less. The 0.74 factor will probably work over a pretty wide range of pointing, but this should be checked.

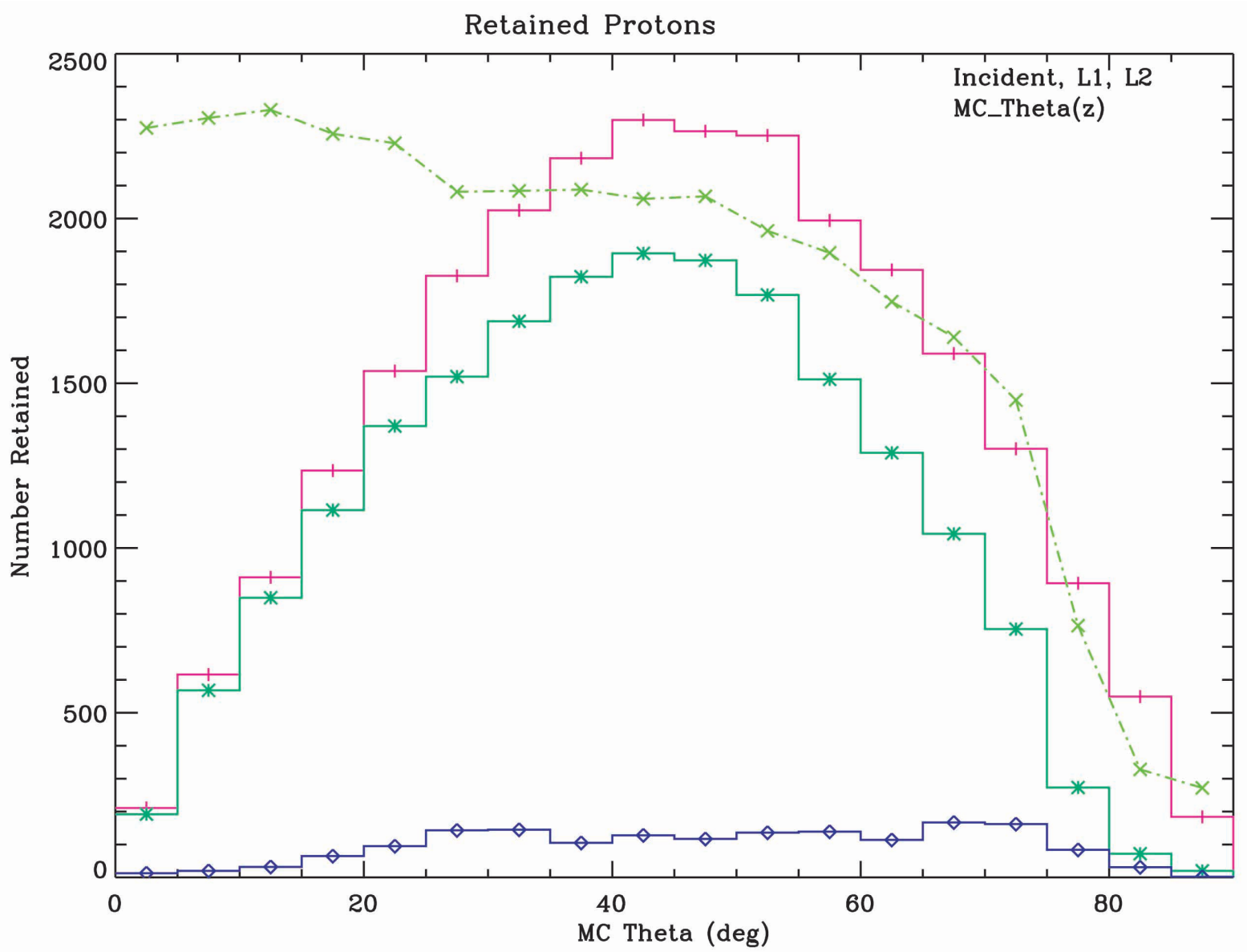

Figure 12a: Zenith angle distributions for particles incident on the top of GLAST and for those selected by the L1 and L2 trigger criteria.

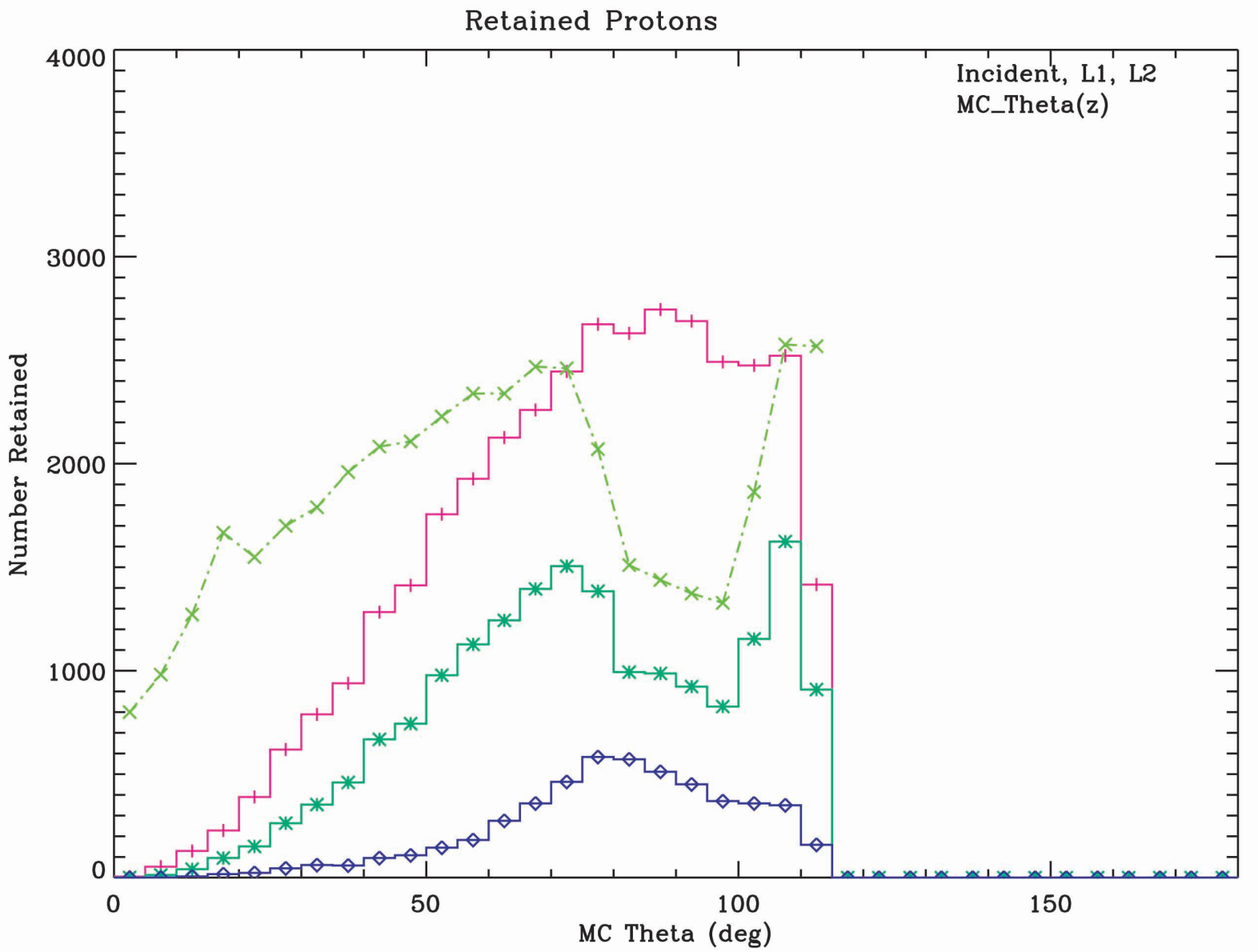

Figure 12b: Zenith angle distributions for particles incident on the side of GLAST and for those selected by the L1 and L2 trigger criteria.

These numbers are derived from the geometric factors given above and the event fractions based on the 5×5 tower array simulations by Norris et al., the results of which are shown in Table 1 and Table 2 for protons and electrons, respectively.

The maximum and orbital average rates of "$E_{cal} > E_{low\text{-}threshold}$" will be threshold dependent; with a threshold at 3 GeV the rates will be approximately the same as those given above. Roughly half of the background events will give a "3-in-a-row" trigger and pass through the calorimeter. Approximately 1/3 of them also deposit "$E_{cal} > E_{low\text{-}threshold}$" in the calorimeter. Most will hit an ACD tile somewhere with a nearby "3-in-a-row" trajectory pointing to it.

The electron spectrum is given in Figure 13. The flux of electrons (E > 3 GeV), 10 /(m^2 sr s), will intersect GLAST at the rate (9.1+14.5) m^2 sr $\times$ 10 electrons /(m^2 sr s), for about 235 Hz. Approximately 2/3 of these will have "3-in-a-row" signatures. The orbital average rate will be 30 - 35 Hz. At flux maximum, electrons trigger at a rate of ~ 25 Hz without making a "3-in-a-row." More than 90% of these electrons enter through the sides or bottom of GLAST and hit the calorimeter. The side anti and its segmentation will be critical for these events. In any case, for our purposes, since there is no defined track in the tracker, we cannot check the ACD tiles at L2, and must defer dealing with these events until L3 or the ground.

We set the ACD inefficiency specification to be $< 3 \times 10^{-4}$, so the rate of protons making "3-in-a-row" and "no.ACD.hit" for $E < E_{low\text{-}threshold}$ will be a maximum of $3 \times 10^{-4} \times 12.7$ kHz = 4. Hz. Rate of electrons making "3-in-a-row" and "no.ACD.hit" for $E < E_{low\text{-}threshold}$ is two orders of magnitude lower.

The differential flux of C-O nuclei (see Figure 14) at 10.6 GeV/nucleon is 7.2×10^{-2} (m^2 s sr GeV/nucleon)$^{-1}$ (E/10.6 GeV/nucleon)$^{-2.7}$. The maximum integral flux of Z = 6-8 nuclei above 1.27 GeV/nucleon is 8 C-O particles per (m^2 sr s). The rate of C-O triggers in the top layers of the ACD will be 1.7×1.7 $m^2 \times \pi$ sr $\times$ 8 (m^2 sr s)$^{-1}$ = 72 Hz. We may wish to restrict this rate by requiring we that accept only those C-O events that deposit $E > E_{low\text{-}threshold}$ in the calorimeter. The geometry for this is about 3.9 m^2 sr and the corresponding rate is 32 Hz, still significant. We can adjust this rate as required for the calibration of the calorimeter by selecting triggers from a subset of tiles or by sampling. We do have to be careful to make the trigger for these events in the calorimeter so it does not affect the measurement.

All these rate estimates are summarized in Table 3.

If we reject all events with a "3-in-a-row" that points back to a hit.ACD, what is the loss of photons due to rejection of all towers by any single tower? Chance rates of two cosmic rays in 1 microsecond:

Maximum: 2×10^{-6} s $\times$ 12.7k Hz $\times$ 12.7k Hz = 320 Hz
Average: 2×10^{-6} s $\times$ 2.6 k Hz $\times$ 2.6 k Hz = 15 Hz
A cosmic ray and a photon: 2×10^{-6} s $\times$ 2.6 k Hz $\times$ 15-30 Hz $\leq$ 0.1-0.2 Hz.

The average chance rates represent a 1% or less loss of signal. Thus, even if any tower can veto the entire instrument at L2, there are no problems created by these chance coincidences.

Assuming we adopt something like the L2 trigger proposed above, at Level 3 or on ground we will need to reject many kinds of residual backgrounds. A few examples are given below.

Reject background from events with "3-in-a-row" .and. "no.ACD.hit"

- single prong events in tracker
- too many "tracks" in tracker
- other "unreconstructables" as pairs
- photons coming from the Earth's limb

Reject background from events with "$E_{cal} > E_{low\text{-}threshold}$"

Calorimeter cuts:

- Shower not electromagnetic in shape, starting point too deep
- Shower comes from bottom or side of calorimeter
- Shape of "cigar" has insufficient length in calorimeter
- Shape of "cigar" is undefined or has too large an error at ACD
- Aspect ratio of "cigar" – too fat for its energy (hadronic vs. electromagnetic showers)

Tracker cuts:

- If tracker track points back to lit ACD tile without at least one unlit tracker layer between (this set may still have some background, but we can check by upping requirement to include not 1 but 2 tracker layers).
- Maybe need to reject events that don't have paired tracks or time-over-threshold for two particles to remove vestiges of e^- events leaking through

ACD. Probably have to consider more than one ACD tile for those events whose point back is near boundary of two (or more) ACD titles. Point back includes "cigar" in calorimeter with at least 2 consistent tracker layer hits (may need 3 tracker hits in straight line). We can use the 2 (or 3) tracker hits to define the ACD tile to check.

Combination cut:

- Calorimeter "cigar" points to tracker but the two trajectories are inconsistent.

These cuts and their efficacy as a function of energy will be discussed elsewhere. Norris and others are working hard to improve their efficacy for both background rejection and photon retention.

Summary

It is hoped that this note will clarify and document the specification of the background rejection problem for GLAST and tie that to the specifications for the ACD rejection of charged particles. We have also tried to clarify the various cosmic ray fluxes and rates involved. The numbers given here have been developed using the 5×5 tower configuration and should be redone in the 4×4 configuration before they are used in the proposal. That will be straightforward once we decide on the L2 trigger criteria. More strict tracking algorithms now being developed by Toby and others should improve the ability to find the tile through which the charged particles passed and reduce the L2 rates.

Comments and corrections to Jonathan F. Ormes at
jfo@LHEApop.gsfc.nasa.gov

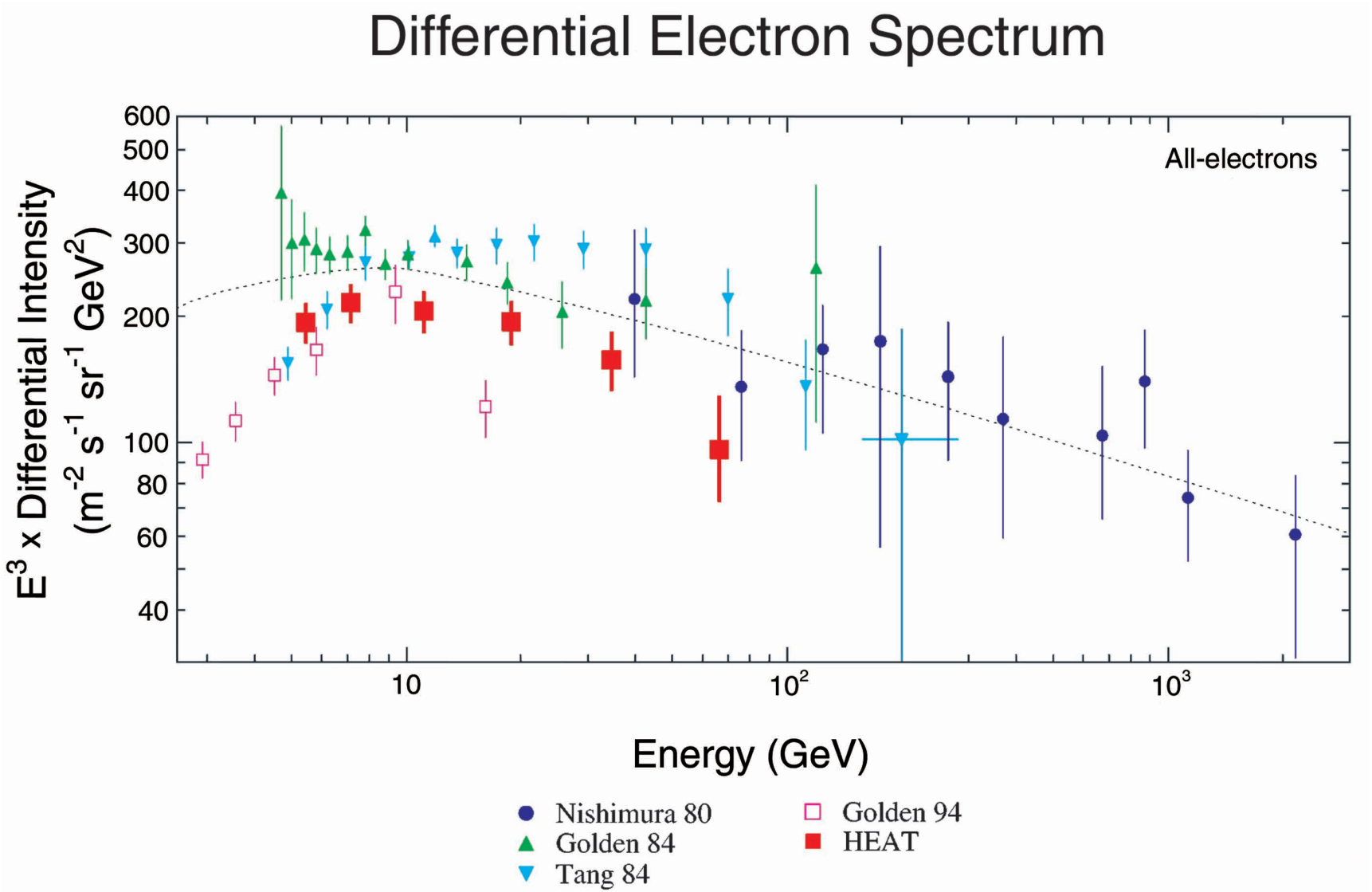

Figure 13: Differential electron spectrum (Barwick, S.W., et al., ApJ, 498, 779 (1998)), see also Taira, et al., XXIII ICRC, Calgary, 2, 128 (1993).
Differential: $I(E)=0.06E^{-3.3}$ $(cm^2\ s\ sr\ GeV)^{-1}$
Integral: $I(E)=0.026E^{-2.3}$ $(cm^2\ s\ sr)^{-1}$

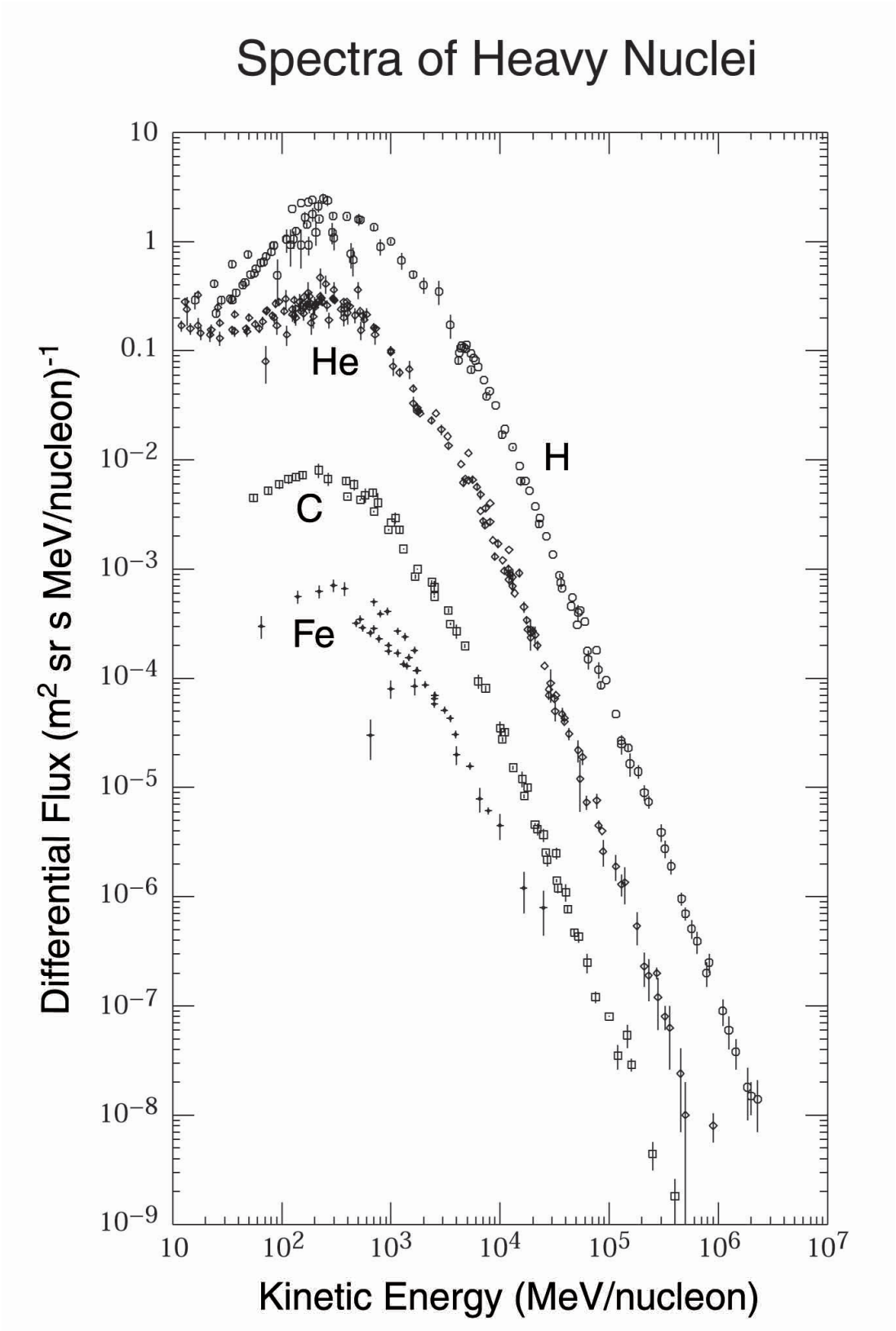

Figure 14: Spectra of heavy nuclei from Particle Data, Simpson, J.A., Ann. Rev. Nucl. & Particle Science, 33,323(1983).

Table 1: Simulations for Protons Selected from the power law spectrum (Figure 2), showing what happens to top entering and side entering events.)

***** Fraction: Retained / Total Incident *****

	L1T TKR	L2T TKR	L1T CAL	L1T C&T	L2T C&T &No ACD	L2T CAL only	Total L1T	Total L2T
(A)	**0.762**	**0.066**	**0.263**	**0.261**	**0.034**	**0.001**	**0.763**	**0.067**
(B)	**0.547**	**0.115**	**0.214**	**0.200**	**0.059**	**0.014**	**0.561**	**0.130**
(C)	**0.549**	**0.154**	**0.303**	**0.216**	**0.127**	**0.087**	**0.636**	**0.241**
(D)	**0.491**	**0.129**	**0.344**	**0.256**	**0.116**	**0.088**	**0.579**	**0.217**
(E)	**0.745**	**0.122**	**0.442**	**0.404**	**0.112**	**0.038**	**0.784**	**0.160**

These fractions are then multiplied by their respective geometry factors, listed below, and by a maximum (average) electron flux of 10 (2) m^{-2} sr^{-1} s^{-1}, to yield the rates in the two subtables at the bottom of the page. Whereas the illumination scheme was 4π uniformly isotropic – designed to test GLAST's defenses from all directions – the geometry factors were calculcate for the respective faces for zenith-pointed mode, with nominal Earth shadowing (the zone $113° < \theta < 180°$ was excluded from the geometry factor weighting for the sides and the bottom of the instrument).

Region of Instrument:		Geometry Factor (m^2 sr)
(A) 51.6 < z < 52.0 (cm)	:TKR Top	9.08
(B) 3.5 < z < 51.6	:TKR Side	7.60
(C) -11.6 < z < 3.5	:Gap Side	2.39
(D) -31.2 < z < -11.6	:CAL Side	3.10
(E) -31.6 < z < -31.2	:CAL Bottom	1.39

column 5: L2T for (CAL .and. TKR) .and. (no ACD veto)
column 6: CAL-only = column 3 - column 4
column 7: L1T total = sum: columns 1 & 6
column 8: L2T total = sum: columns 2 & 6

***** Maximum Proton Rates (Hz) at L1T and L2T *****

	(A) TKR Top	(B) TKR Side	(C) GAP Side	(D) CAL Side	(E) CAL Bot	Total
L1T:	**6238**	**3838**	**1369**	**1616**	**980**	**14040**
L2T:	**551**	**886**	**518**	**604**	**201**	**2760**

***** Average Proton Rates (Hz) at L1T and L2T *****

	(A) TKR Top	(B) TKR Side	(C) GAP Side	(D) CAL Side	(E) CAL Bot	Total
L1T:	**1296**	**797**	**284**	**336**	**204**	**2917**
L2T:	**114**	**184**	**108**	**126**	**42**	**573**

Table 2: Simulations for Electrons Selected from $E^{-3.3}$ Power Law (Figure 4), showing what happens to top entering and side entering events.)

***** Fraction: Retained / Total Incident *****

	L1T TKR	L2T TKR	L1T CAL	L1T C&T	L2T C&T &No ACD	L2T CAL only	Total L1T	Total L2T
(A)	**0.766**	**0.041**	**0.443**	**0.442**	**0.012**	**0.001**	**0.767**	**0.042**
(B)	**0.615**	**0.141**	**0.273**	**0.231**	**0.025**	**0.043**	**0.658**	**0.183**
(C)	**0.524**	**0.185**	**0.402**	**0.102**	**0.099**	**0.300**	**0.824**	**0.486**
(D)	**0.322**	**0.124**	**0.614**	**0.171**	**0.108**	**0.443**	**0.765**	**0.567**
(E)	**0.432**	**0.221**	**0.880**	**0.405**	**0.219**	**0.475**	**0.906**	**0.696**

These fractions are then multiplied by their respective geometry factors, listed below, and by a maximum (average) electron flux of 10 (2) m^{-2} sr^{-1} s^{-1}, to yield the rates in the two subtables at the bottom of the page. Whereas the illumination scheme was 4π uniformly isotropic – designed to test GLAST's defenses from all directions – the geometry factors were calculcate for the respective faces for zenith-pointed mode, with nominal Earth shadowing (the zone $113° < \theta < 180°$ was excluded from the geometry factor weighting for the sides and the bottom of the instrument).

Region of Instrument:		Geometry Factor (m^2 sr)
(A) 51.6 < z < 52.0 (cm)	:TKR Top	9.08
(B) 3.5 < z < 51.6	:TKR Side	7.60
(C) -11.6 < z < 3.5	:Gap Side	2.39
(D) -31.2 < z < -11.6	:CAL Side	3.10
(E) -31.6 < z < -31.2	:CAL Bottom	1.39

column 5: L2T for (CAL .and. TKR) .and. (no ACD veto)
column 6: CAL-only = column 3 - column 4
column 7: L1T total = sum: columns 1 & 6
column 8: L2T total = sum: columns 2 & 6

***** Maximum Electron Rates (Hz) at L1T and L2T *****

	(A) TKR Top	(B) TKR Side	(C) GAP Side	(D) CAL Side	(E) CAL Bot	Total
L1T:	**70**	**50**	**20**	**24**	**13**	**176**
L2T:	**4**	**14**	**12**	**18**	**10**	**57**

***** Average Electron Rates (Hz) at L1T and L2T *****

	(A) TKR Top	(B) TKR Side	(C) GAP Side	(D) CAL Side	(E) CAL Bot	Total
L1T:	**14**	**10**	**4**	**5**	**3**	**35**
L2T:	**1**	**3**	**2**	**4**	**2**	**11**

Table 3: A Summary of the Rates in This Note

	Maximum (Hz)	Average (Hz)
L1:		
protons "3-in-a-row"	13450	2800
electrons "3-in-a-row"	145	30
noise	100	100
"$E_{cal} > E_{low\text{-}threshold}$" (only)	620	130
"$E_{cal} > E_{high\text{-}threshold}$"(included above)	(50)	(50)
limb photons	240	120
sky photons	15	10
Hi-Z triggers	70	20
L1 Total	14640	3210
L2:		
protons "3-in-a-row" (wrong ACD)	2170	450
electrons "3-in-a-row" (wrong ACD)	25	5
noise	100	100
"$E_{cal} > E_{low\text{-}threshold}$" (only)	620	130
"$E_{cal} > E_{high\text{-}threshold}$"(included above)	(50)	(50)
limb photons	240	120
sky photons	15	10
Hi-Z triggers	70	20
L2 Total	3240	835
Leakage through failed ACD tile	260	60
Total with Failed ACD tile	2600	700

IDL Program to calculate Geometric factor of two coaligned rectangles.
J. D. Sullivan, 1971, NIM 95, 5 and errata.

The upper rectangle has dimensions a1 x b1, the lower a2 x b2.
Their separation is h.

Function Sullivan, a1, b1, a2, b2, h

```
alpha = (a1+a2)/2.
beta = (b1+b2)/2.
gamma = (a1-a2)/2.
delta = (b1-b2)/2.
temp1 = h*h + alpha*alpha
temp2 = h*h + gamma*gamma
temp3 = h*h + beta*beta
temp2 = h*h + delta*delta
stemp1 = sqrt(h*h + alpha*alpha)
stemp2 = sqrt(h*h + gamma*gamma)
stemp3 = sqrt(h*h + beta*beta)
stemp4 = sqrt(h*h + delta*delta)
rat1 = (temp1 + delta*delta)/(temp1 + beta*beta)
rat2 = (temp2 + beta*beta)/(temp2 + delta*delta)
t1 = h*h*alog(rat1*rat2)
t2 = 2.*alpha*stemp3*atan(alpha/stemp3)
t3 = 2.*beta*stemp1*atan(beta/stemp1)
t4 = -2.*alpha*stemp4*atan(alpha/stemp4)
t5 = -2.*beta*stemp2*atan(beta/stemp2)
t6 = -2.*gamma*stemp3*atan(gamma/stemp3)
t7 = -2.*delta*stemp1*atan(delta/stemp1)
t8 = 2.*gamma*stemp4*atan(gamma/stemp4)
t9 = 2.*delta*stemp2*atan(delta/stemp2)

return, t1+t2+t3+t4+t5+t6+t7+t8+t9

end
```